63-3-3

ASD-TDR-62-1067

STUDIES OF HYDROGEN AND OXYGEN EVOLUTION AND THE INFLUENCE OF ABSORBED SUBSTANCES

TECHNICAL DOCUMENTARY REPORT NO. ASD-TDR-62-1067

March 1963

Directorate of Materials and Processes
Aeronautical Systems Division
Air Force Systems Command
Wright-Patterson Air Force Base, Ohio

Project Nos. 7022, 7353, Task No. 735305

(Prepared under Contract No. AF 61(052)-305
by the Technische Hochschule, Munich, Germany;
L. Kandler, H. Bickl, H. Feigl, and E. Heusler, authors.)

NOTICES

When Government drawings, specifications, or other data are used for any purpose other than in connection with a definitely related Government procurement operation, the United States Government thereby incurs no responsibility nor any obligation whatsoever; and the fact that the Government may have formulated, furnished, or in any way supplied the said drawings, specifications, or other data, is not to be regarded by implication or otherwise as in any manner licensing the holder or any other person or corporation, or conveying any rights or permission to manufacture, use, or sell any patented invention that may in any way be related thereto.

Qualified requesters may obtain copies of this report from the Armed Services Technical Information Agency, (ASTIA), Arlington Hall Station, Arlington 12, Virginia.

This report has been released to the Office of Technical Services, U.S. Department of Commerce, Washington 25, D.C., in stock quantities for sale to the general public.

Copies of this report should not be returned to the Aeronautical Systems Division unless return is required by security considerations, contractual obligations, or notice on a specific document.

26-619C, 700, 9-1-6

FOREWORD

This report was prepared by the Technische Hochschule, Munich, Germany, under USAF Contract No. AF 61(052)-305. This contract was initiated under Project 7022 and later redocumented under Project 7353, "Characterization of Solid Phase and Interphase Phenomena in Crystalline Substances," Task 735305 "Interactions and Reactions Occurring at Interfaces." The work was administered under the joint direction of Directorate of Materials and Processes, Aeronautical Systems Division and the European Office, Air Force Systems Command, with Dr. R. J. Barton succeeded by Lt. John J. Reishus acting as project engineer.

This report covers work conducted from 1 March 1961 to 28 February 1962.

ABSTRACT

This investigation has been concerned with Hydrogen and Oxygen Evolution at electrodes and the influence of adsorbed substances. In this report AC measurements of the interface impedance prove to be suitable for studying adsorption phenomena on porous electrodes like platinated platinum and sintered nickel material. The impedance on platinum electrodes was evaluated for 8N H_2SO_4 an IN KOH solutions. Further investigations dealt with inhibition problems on highly activated porous nickel electrodes. Several alcohols were used as additives to IN KOH.

The applicability of the potentiostatic method of applying triangular voltages was examined on bright nickel electrodes. The electrolytes 8N H_2SO_4 in IN KOH in general were stirred with purified nitrogen. The applicability of the potentiostatic method of triangular voltages to show the influence of inhibitors by applying the principle of Wagner-Traut was examined.

This technical documentary report has been reviewed and is approved.

E. M. KENNEDY, Jr. Lt. Col. USAF
Chief, Advanced Metallurgical Studies Branch
Metals and Ceramics Laboratory
Directorate of Materials and Processes

Contents

page

Part I

1. Summary

In this report A.C.-measurements of the interface impedance prove to be suitable for studying adsorption phenomena on porous electrodes like platinated platinum and sintered nickel material. In order to get a close connection between previous investigations on bright platinum wire electrodes and highly porous nickel electrodes, at first the impedance on platinated platinum electrodes was evaluated for 8N H_2SO_4 and 1N KOH solutions. For both hydrogen bubbled electrode systems, activated porous nickel and activated bright or platinated platinum similar electrochemical reactions could be found. There is a reversible build-up of the hydrogen potential, a limiting anodic diffusions current of molecular hydrogen, a catalytic dissociation reaction on the surface, and adsorption of hydrogen atoms.

Further investigations dealt with inhibition problems on highly activated porous nickel electrodes. Several alcohols like methanol, aethanol, n-butanol, isobutanol, glycol, and glycerin, which could be partly dehydrogenated, were used as additives to 1N KOH. Steady-state current-voltage curves for both, the anodic and cathodic, ranges of potentials were recorded under potentiostatic conditions. A.C.-measurements of the electrochemical impedance were limited to potential range of hydrogen adsorption. Additives of glycol or glycerin cause interruption of hydrogen evolution at negative potentials due to a complete inhibition. If negative potentials are increased the inhibition can be cancelled again. If charged at positive potentials the activity of the nickel electrode is reduced by oxydation products of the alcohols added. The reversible hydrogen adsorption gets also inhibited in part. Aethanol as an additive to 1N KOH represents an exception.

2. General Remarks on the A.C.-Method

In the reports submitted so far (Contr. No. AF 61 (052)-142; Contr. No. AF 61 (052)-352) the method of applying triangular voltages was used for the research on the H_2 and O_2 adsorption and desorption at bright surfaces of noble metal electrodes. The measurement of phase impedance, however, has proved to be of advantage for the research on the adsorption and desorption in porous electrodes. Besides, this method yields more detailed results on the kinetics of electrode processes.

Manuscript released by authors 7 January 1963 for publication as an ASD Technical Documentary Report.

In applying the phase impedance measurements alternating currents of small amplitudes and variable frequencies (5 cps to 10 cps) are superposed the direct currents of electrolysis. In an AC circuit the surface of the test electrode is represented by an ohmic and a capacitive component. This complex resistance (impedance) is determined physically by the kinetic processes at the interface between electrode metal and electrolyte. Therefore, conclusions to the kinetics of the electrode processes can be drawn from both, its value and its dependence from the frequency and overvoltage.

Impedance measurements show two characterizing features of the test electrode; one term resembles the electrostatic double layer impedance, the other is due to the charge transfer across the double layer. Both, the double layer impedance and the ohmic resistance of the electrolyte, also shown in the measurement, have to be seperated. At the electrode the alternating current splits into two components, i_D, the charging current of the double layer impedance and i_F, the current representing the discharge. Therefore, an equivalent circuit diagram consisting of two complex resistances connected in parallel, can be drawn for the electrode. The values of impedances resulting from the charge-transfer and corresponding thereby to the actual electro-chemical reaction generally consist of several capacitive and ohmic resistances, which usually also depend on frequency.

In the case of the hydrogen adsorption and desorption the transfer current i_F is a function of the applied voltage U and the concentration of the atomic hydrogen c_H, adsorbed on the surface of the electrode.

$$i_F = f(U c_H)$$

According to Grahame [1] there is

$$\Delta i_F = \left(\frac{\partial i_F}{\partial U}\right)_{c_H} \cdot \Delta U + \left(\frac{\partial i_F}{\partial c_H}\right)_U \cdot \Delta c_H$$

Δc_H and ΔU represent the changes of c_H and U caused by the alternating current i_F.

The transfer impedance $R_F = \frac{\Delta U}{\Delta i_F}$ derived therefrom is

$$R_F = \left(\frac{\partial U}{\partial i_F}\right)_{c_H} - \left(\frac{\partial U}{\partial i_F}\right)_{c_H} \cdot \left(\frac{\partial i_F}{\partial c_H}\right)_U \cdot \frac{\Delta c_H}{\Delta i_F}$$

This shows that R_F consists of two components. The first term is ohmic because it corresponds to Voltage changes at flowing current and a given concentration of c_H. The second term is of a complex capacitive nature since changes in the concentration c_H lag behind the alternating current applied, thus causing pseudo-capacities.

3. Apparatus Used for A.C.-Measurements

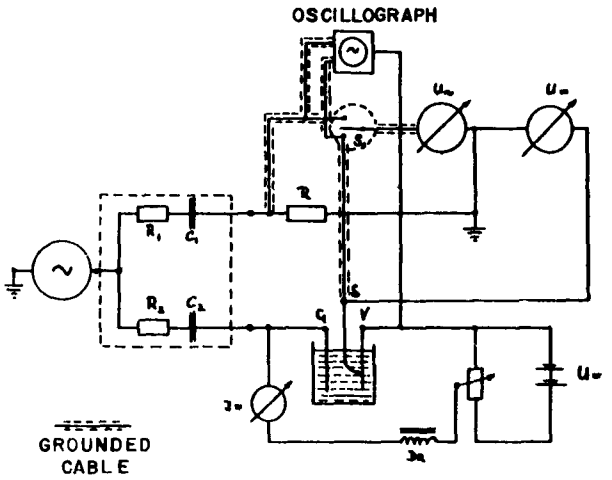

Figure 1

In figure 1 the a-c and d-c circuit of the experimental device is shown. A-c is supplied by an a-c-generator. Frequency and amplitude can be changed. A-c is divided into two branches, one of which contains the test vessel, the other is represented by the resistor R evaluated to 0.5% accuracy. R was a suitable one of a set of standard resistors. The two resistors R_1 and R_2 connected in series to the cell and standard R respectively are equal to each other and essentially higher dimensioned than R. Together with the two capacitors C_1 and C_2, which are again equal of value, this device causes equal amounts of a.c. to flow with equal phase shift through the test vessel and the standard resistor R used for measurements. By changing the out-put voltage of the generator a.c. always can be chosen so, that there are exactly 5 mV between the test electrode V and the probe S. The absolute amount of the impedance can be calculated from this voltage, the voltage U_R across R, and the standard resistor R, according to

$$\mathcal{R} = \frac{U}{U_R} \times R$$

R is provided in the same order of magnitude as $\mathcal{R}$.

The phase lag φ of the electrode impedance is evaluated with the aid of a Tektronix 502 Dual-Beam Oscilloscope, which serves as a two channel X-Y recorder. For that purpose the a.c voltage across the standard resistor R is applied the horizontal deflection system, a.c. voltage taken between the test electrode V and the probe S is connected to the vertical deflection system of the oscilloscope. From the photographed ellipsis on the screen the phase shift φ between both the a.c. voltages is calculated.
For d.c. charging of the test electrode a potentiometer circuit with low internal resistance is used, which provides the applying of constant voltages to the test electrode. A sufficiently high dimensioned inductance (132 hy, 200 Ω) is inserted in the d.c. circuit and prevents a.c. from flowing in parallel to the test vessel.

Since the impedances of the electrodes measured by us is about 1 Ω great precautions have to be taken in circuiting. Otherwise the results would be greatly distorted by hum and phase lags. Troubles caused by jitter and hum voltages across the test cell can be minimized to 20 μ V by short low-resistance leads and polished plugs, which have to be replaced sometimes. Shielded leads yield no further decrease of the interfering voltage. Shieldings are only wanted for the leads connecting the a.c. instruments to the actual test device.

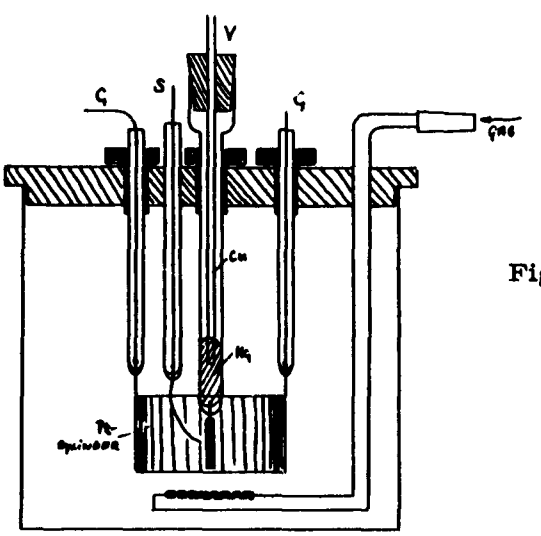

Figure 2

Figure 2 shows the test vessel. The test electrode V connected to ground is situated in the axis of a cylindrical electric field. The Electrode materials investigated, like platinated platinum wires and little sheets of porous highly activated nickel, are welded on links of platinum, to which narrow glass tubes are melted. In case of testing nickel electrodes, remaining platinum surfaces exposed to the electrolyte are thoroughly covered with a special lac. In order to get a minimum of ohmic resistance, electric contacting is done by mercury and a 4 mm diameter wire of copper. A large cylinder G of platinum is used as a counter-electrode for a.c. and d.c. The point of this platinated platinum wire S is located as close as possible to the surface of the test electrode to minimize the ohmic drop caused by the electrolyte. This device is suitable as a reference electrode and moreover as a probe for measuring the impedances. Thus only the impedance of the test electrode and a small amount of the electrolytic resistance between the test electrode and the probe are recorded. The impedance of the counter-electrode must not be taken in account.

Gas bubbling is done with the aid of a sintered glass disk (fritte).

4. Impedance Measurements of the Interface Between Platinated Platinum Electrodes and 8N H_2SO_4 and 1N KOH

4.1 Experimental Results.

According to a previous chapter, the investigations on platinated platinum electrodes were performed to get a closer connection between the kinetics of bright platinum electrodes already known and the more interesting problems concerning highly activated porous nickel electrodes. The interpretation of the test results, obtained on platinated platinum surfaces in 8N sulphuric acid and 1N KOH proved to be possible according to the theories of Dolin-Ershler [2] and Breiter-Warburg [3,4], which already have been derived for bright surfaces of noble metals in acid solutions.

4.1.1 Results for Platinated Platinum in 8N H_2SO_4.

In order to get the results reproduced the electrode was polarized for 5 minutes by applying a voltage of +1200 mV. Subsequently, hydrogen-bubbling led to an open-circuit build-up of the reversible hydrogen potential. During the measurements constant hydrogen pressure was maintained for stirring the electrolyte.

The apparent geometrical surface of the electrode was f = 0.087 cm^2. The impedance was recorded as a function of the potential for various frequencies of the a.c. superposed.

Converting the impedance to the terms of a connection in parallel provides the capacities C_P plotted vs. potential U, as shown in figure 3a.

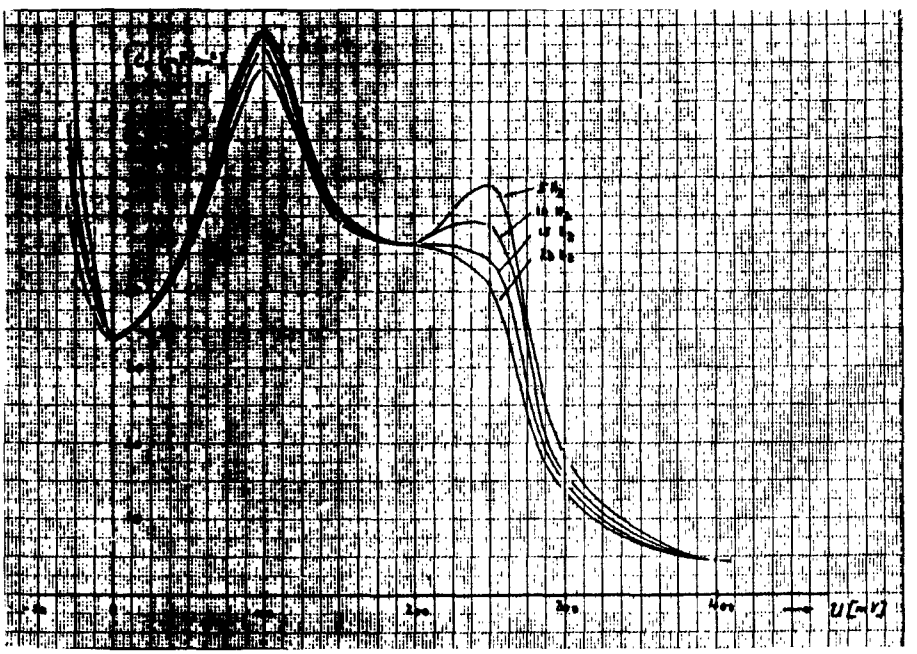

Figure 3a

The course of the curve is characterized by two maxima at U = +100 mV and U = +250 mV. For bright platinum surfaces curves of the same shape have already been found by Breiter, Kammermeier, and Knorr [3]. Other measurements by Knorr, Breiter, and Will [5] or Breiter and Böld [6] as well as Breiter and Kennel [7] proved similar results for bright surfaces by applying the triangular pulsemethod. The C_P-U-curve for platinated platinum resulting from our test differs in the first minimum at the capacity C_P from the curves described by the authors above. According to these investigations on bright platinum surfaces this minimum is found at U = +50 mV if low frequencies are applied. Only using higher frequencies causes a shift to more negative potentials. In our tests on platinated platinum, however, this minimum was found already at U = O mV applying a frequency of 5 c.p.s. Besides, there is an other difference concerning the potential of

C_p-maximum which is found to be shifted from +200 mV to +250 mV. These measurements are performed on platinated platinum instead of bright platinum surfaces. A sharp rise of C_p-values at negative potentials is due to molecular hydrogen, large amount of which must be adsorbed on highly roughened surfaces to meet the pressure of hydrogen atmosphere.

The dependence on frequency of the imaginary component C_p of the impedance resulting for the potential range between U = -50 mV and U = +40 mV is plotted in figure 3b (C_p vs. $\omega^{-1/2}$).

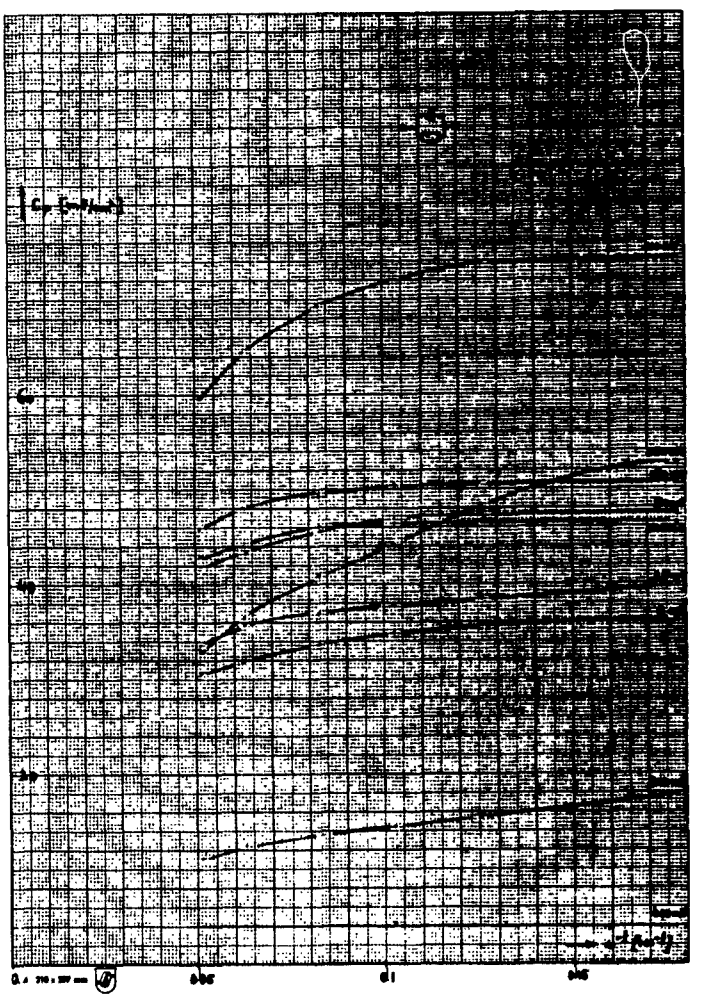

Figure 3b

For small frequencies C_p tends to a limiting value, which depends on the voltage applied according to a decrease with potentials exceeding +300 to more positive values. These limiting values correspond to the pseudo-capacities C_2 of adsorbed hydrogen atoms. Finally at U = +400 mV there is only little difference between the C_p's evaluated for 5 c.p.s. and 10 kc.p.s. This value may be due to the double layer capacity. Applying small frequencies for the range between U = -50 mV and U = +25 mV the resulting C_p, $\omega^{-1/2}$-curves yield straight lines, which correspond to a diffusion controlled process. According to Kammermeier, Breiter, and Knorr [3] this is conditioned by the diffusion of molecular hydrogen.

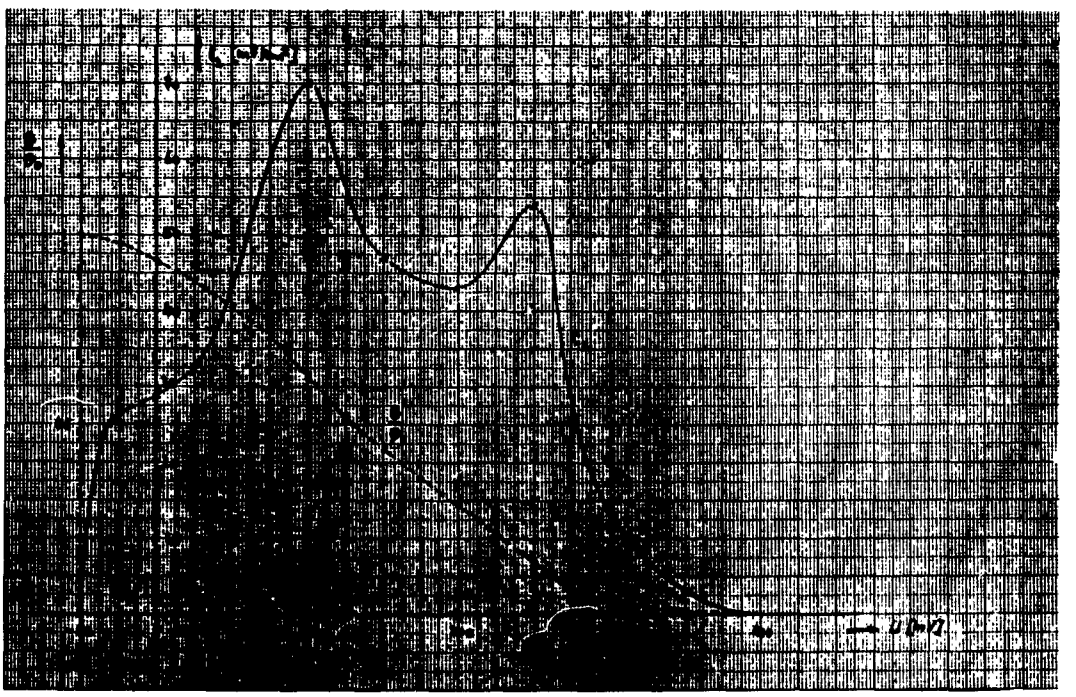

Figure 3c

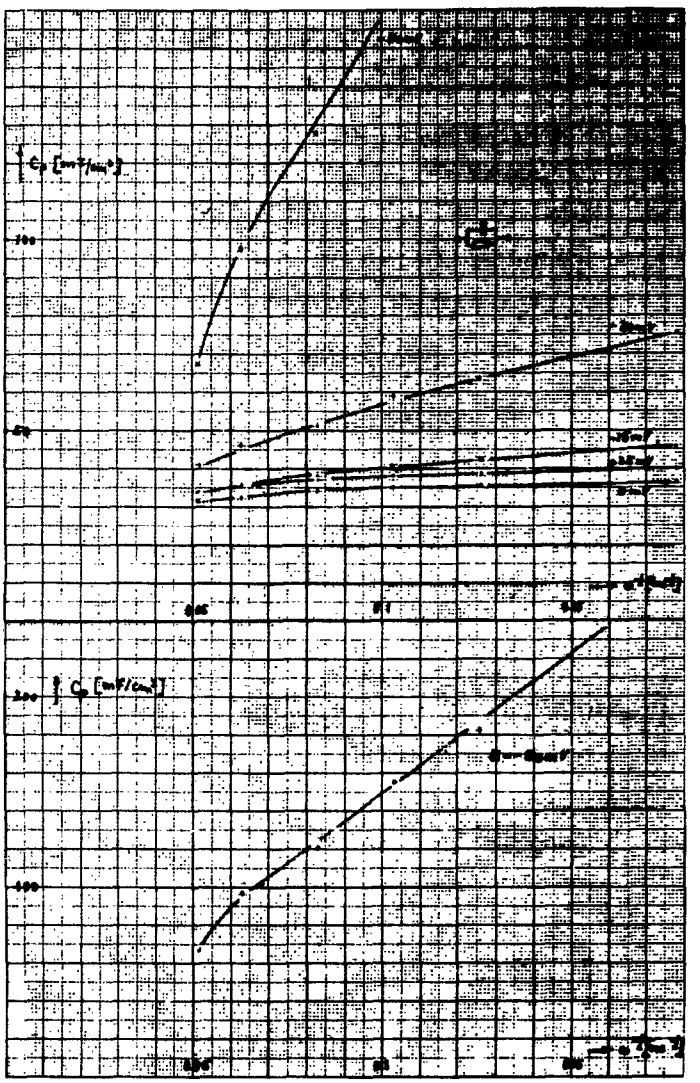

Figure 3d

As shown in figure 3c, the pseudo-capacity C_2 of the adsorbed atomic hydrogen and the ratio of hydrogen coverage vs. voltage U. For the range of potentials between -50 mV and +25 mV C_2 is evaluated from the plots of figure 3d by extrapolating the linear C_P-$\omega^{-1/2}$-function obtained for low frequencies to $\omega = \infty$. (Reference is made to the theories of Breiter and Warburg) [3,4]. Thus the influence of adsorbed molecular hydrogen joining the measurements of C_P could be eliminated. C_2 equals zero at U = -50 mV in contrast to the results recorded on bright platinum electrodes. This explains also the shift of the first capacity

minimum of the C_p-U-curve to more negative potentials in case of platinated platinum. C_2 for the range of potentials between +50 mV and +300 mV is evaluated from the constant C_p value for small frequencies according to the theory of Dolin and Ershler [2] (of. the curves of figure 3b) The C_p's are corrected by subtracting the double layer capacity, represented by a C_p-value independent from frequency at U = +400 mV. The fraction of hydrogen coverage Θ as a function of the applied potential is calculated by a stepwise graphic integration of the C_2-U-curve (of Eucken and Webus [8]). The resulting curve is normalized in a way that unit 1 is set up for this fraction Θ_o of hydrogen coverage which tends to a limit at U = -50 mV. A complete coverage of the surface of the electrode is assumed applying this voltage.

4.1.2 Results for Platinated Platinum in 1N KOH

The measurements on platinated platinum in alkaline solutions cannot as easily be explained according to the theories of Dolin-Ershler [2] and Breiter-Warburg [3,4] as the measurements concerning 8N H_2SO_4. A diffusion process disturbes the results up to U = +400 mV. According to Slygin [9] and Dolin-Ershler [2] this diffusion process is the surface diffusion of adsorbed atomic hydrogen. The authors could also observe this effects testing bright surfaces of platinum electrodes. For our investigations again a platinated platinum wire was used. It was especially carefully activated since platinum surfaces are quickly disactivated in alkaline solution.

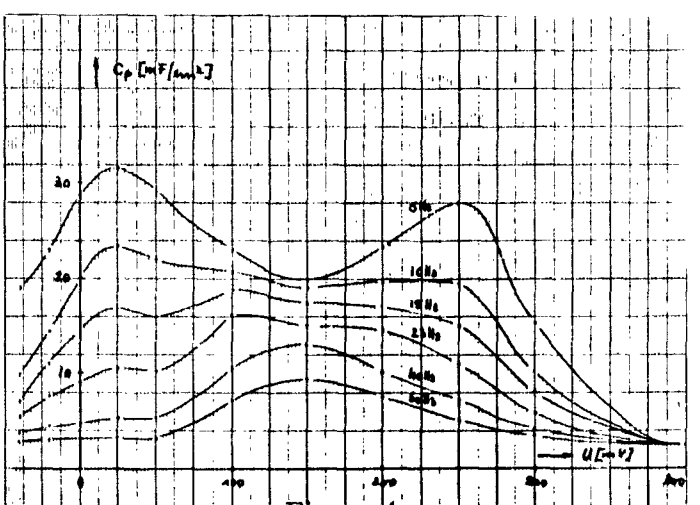

Figure 4a

Figure 4a shows the dependance of C_p on the overvoltage U at different frequencies. At lower frequencies the curves show two distinct maxima at U = +25 mV and U = +250 mV which change their shapes applying higher frequencies. Finally there is only one maximum at U = +150 mV. This curve showing two maxima is only known on platinum in acids, but has not yet been found in alkaline solutions. It is only through our special method of measuring impedances of interfaces that the impedance can be analysed as far down as 5 cps. At higher frequencies the wellknown (Cf Dolin-Ershler [2] and Franke, Knorr, Breiter [10]) single maximum appears in our tests at U = +150 mV, too. The determination of C_2-values at a range of voltages between +100 mV and +400 mV according to the theory of Dolin-Ershler [2] is possible only if C_p for the frequency f = 0 cps is taken by extrapolation. Between -50 mV and +50 mV C_2 is determined in accordance with the theory of Breiter-Warburg which can be applied unrestrictedly. According to this theory, C_2 results from an extrapolation of the C_p values to the frequency $f = \infty$ cps. Diffusion processes have no influence on this value. Figure 4b shows the C_2-U-curve resulting therefrom and the Θ-U-curve obtained from a stepwise graphic integration. The Θ value at U = -50 mV is the unit Θ_o for the $\frac{\Theta}{\Theta_o}$-U-curve.

Figure 4b

As experiences so far have shown this method can be applied to other porous electrode materials, besides, to problems of specific adsorption (inhibition).

5 Impedance Measurements of the Interface Between Porous Nickel Electrodes in 1N KOH

5.1 Preparation of Highly Activated Electrodes

According to an electrochemical method developed some years ago there is an opportunity to fill up the pores of a nickel skeleton with a highly divided precipitation of $Ni(OH)_2$. Most fitted to preparation are nickel skeleton materials, which consist of perforated foils or fine-meshed nets. On either side carbonyl-nickel powder was sintered to a layer of 0.4 mm thickness. The over-all volume of pores amount to 70%. $Ni(OH)_2$ filling up the pores of the nickel skeleton is reduced in an oven in the presence of a hydrogen atmosphere. Reduction is performed for some hours on a temperature of 200 to 300°C. Porous nickel electrodes prepared as described are excellent catalysts for hydrogenation reactions. In contrast to nickel powder, produced by reduction of cristallized $Ni(OH)_2$ at temperatures between 200 to 300°C, these catalysts, if brought to the open air at room temperature, indicate no pyrophorous attributes. It is not before approxiamtely 80°C that electrodes just reduced show phenomena of a violent oxydation. At room temperature this oxydation is slow and the electrodes loose their activities only gradually. Keeping the plates in KOH provides less lowering of the activity. So after a year there is only a loss of about 30% of the activity of freshly prepared material.

This highly activated nickel was used in part for our investigations. The geometric area of the electrodes was 1 cm^2 on an average. 1N KOH again was used as an electrolyte. In order to get our results reproduced, in the beginning of every series of tests there was an anodic pretreatment with 10 mA/cm^2 for about 12 hours. After this the auxiliary cathode used was removed without cut-off of current. Thus at the same time the electrolyte was purified by pre-electrolysis. By a subsequent cathodic charging of the electrode with small current densities, the oxygen adsorbed during pretreatment was reduced, and, after two or three hours, finally replaced by adsorbed hydrogen. Hydrogen bubbling alone was not sufficient to remove the adsorbed oxygen. After this cathodic pre-electrolysis the reversible hydrogen potential could be maintained for a long time, even without any hydrogen bubbling. This could be controlled by referring to a hydrogen bubbled platinum electrode platinated afresh and immersed into the same electrolyte.

Measurements of the impedance of the electrode could be performed after getting stationary conditions. This was indicated by constant values for the impedance $\mathcal{R}$ and for the current density.

The electrolyte was hydrogen stirred under pressure control.

5.2 Cathodic Hydrogen Over-Potential for Alkaline Solutions

The amount of hydrogen over-voltage necessary for electrochemical hydrogen evolution is highly dependent on the nature of the electrode material and is defined by the kinetics of electrode processes. Bonhoeffer [11] stated in 1924 that hydrogen over-potential decreases the more, the higher the catalytic action of the surface for splitting up the hydrogen molecules can be made. Our highly porous nickel electrodes are excellent catalysts for hydrogen involving reactions. From this it is quite clearly understood that our measurements prove very low hydrogen over-potential.

In alkaline solutions hydrogen development is due to the gross reaction

$$2\ H_2O + 2e^- \longrightarrow H_2 + 2\ OH^-$$

which again consists of a sequence of reaction steps.

Two schemes of reaction sequences are known:
the Volmer [12] Tafel-mechanism and the Volmer-Heyrovsky [13]- mechanism. The Volmer-Heyrovsky - mechanism is characterized by two different succeeding charge transfer reactions according to the equations

$$H_2O + e^- \longrightarrow H_{ads.} + OH^- \qquad \text{Volmer}$$

$$H_{ads} + H_2O + e^- \longrightarrow H_2 + OH^- \qquad \text{Heyrovsky}$$

$H_{ads.}$ stands for the atomic hydrogen adsorbed at the electrode surface.

The Volmer -Tafel mechanism involves two electrons due to the Volmer reaction, which has to act twice. By means of the Tafel-reaction the two adsorbed hydrogen atoms recombine according to

$$2\ H_{ads} \longrightarrow H_2 \qquad \text{Tafel}$$

H.Gerischer [14] stated that the Heyrovsky -reaction is more restrained if the adsorbed hydrogen atom operates stronger building forces versus the surface of the

metal. In this way the Volmer -reaction gets preferred. From our AC measurements can be assumed that the heat of adsorption for atomic hydrogen of platinum equals that of highly activated porous nickel electrodes. This would indicate that there is a complete suppression of the Heyrovsky-reaction. This could be proved by our measurements. For this reason only the kinetics of the Volmer -Tafel-mechanism are discussed in the following chapter.

5.2.1 Theorie of the Volmer-Tafel-Mechanism

For alkaline electrolytes the Volmer -Tafel-mechanism is based on the following reactions

$$H_2O + e^- \longrightarrow H_{ad} + OH^-$$

$$H_2O + e^- \longrightarrow H_{ad} + OH^-$$

$$2\,H_{ad} \longrightarrow H_2$$

The equation of Volmer

$$i = k^+ [OH^-] \cdot \Theta \exp\left(\frac{\alpha F}{RT}\varepsilon\right) - k^- (1 - \Theta) \exp\left(-\frac{(1-\alpha)F}{RT}\varepsilon\right)$$

stands for the discharge reaction

α = Transfer coefficient $(0 < \alpha < 1)$

ε = Potential for the electrode

Θ = fraction for surface covered by atomic hydrogen $(0 < \Theta < 1)$

F = Faradaic coefficient

k^+, k^- = rate constants in units of current density

The first term $i^+(\varepsilon)$ represents the anodic component, the second term $i^-(\varepsilon)$ is due to the cathodic component of the current densities. Equality of there two components yields the exchange current density and characterizes the equilibrium potentials

$$i_o = i^+(\varepsilon) = |i^-(\varepsilon)|$$

introducing the exchange current density i_o and Θ_o the fraction of surface area

covered by hydrogen atoms under equilibrium conditions, gives

$$i = i_o \left[\frac{\Theta}{\Theta_o} \exp \frac{\alpha F}{RT} U - \frac{1 - \Theta}{1 - \Theta_o} \exp \left(- \frac{(1-\alpha)F}{RT} U \right) \right]$$

This represents a normalization of the Volmer equation with respect to i_o. Whereas hydrogen atoms are discharged due to the Volmer-reaction, recombination according to the Tafel-mechanism takes place, if $\Theta > \Theta_o$. Existing a high rate of recombination or applying a high cathodic current, nevertheless $\frac{\Theta}{\Theta_o} \approx 1$ may be valid. At increased cathodic overpotentials the anodic component of the current density may be neglected, thus resulting in

$$U = \frac{RT}{(1-\alpha)F} \ln i_o - \frac{RT}{(1-\alpha)F} \ln |i|$$

which is a Tafel-type equation, where $U = a + b \log i$.
$\alpha = 0.5$ gives $b = 118$ mV for 25°C. The rate of hydrogen discharge discussed here, gets controlled by the Volmer -reaction, concentration polarisation, i.e. if pH around the electrode is independent from the current density i. Thus the overpotential U is merely due to a restraint of charge transfer. If the recombination reaction - a second-order process - is rate determining it can be assumed that the equilibrium of Volmer-reaction is approximately attained. Thus Nernst equation is applicable to the Volmer-reaction

$$\varepsilon = \varepsilon_o + \frac{RT}{F} \ln \frac{1 - \Theta}{\Theta [OH^-]}$$

If Θ_o the ratio of H-coverage at equilibrium is introduced into the equation above the equilibrium potential ε_o can be calculated. Recombination implies $\Theta > \Theta_o$. Only then the rate of the recombination reaction

$$V = k (\Theta^2 - \Theta_o^2) = -iF$$

equals the rate of formation of the H-atoms i.F. By introducing a positive reaction current density i_r according to L.P.Hammet [15] results

$$U = - \frac{RT}{2F} \ln \left(1 - \frac{i}{i_r}\right)$$

which for sufficient high negative overpotentials, i.e. $i \gg i_r$, passes into

an equation, already given by Tafel in 1905:

$$U = +\frac{RT}{2F} \ln i_r - \frac{RT}{2F} \ln |i|$$

This value of b, which amounts to $-\frac{2303}{2F} RF = -29.6$ mV at 25°C, was found for example by Clamroth and Breiter [16] on charging smooth platinum surfaces with small cathodic current densities. Small ratios of $\frac{i_r}{i_o}$ provided, increasing the cathodic current densities results in a continuous change of the slope b = -29.6 mV to be $= -\frac{59.2}{1-\alpha}$ mV. This was also proved by experiments of Clamroth and Breiter et alt.

5.2.2 Experimental Results

Electrodes of highly activated nickel sinter material were investigated using the galvanostatic technique. The apparent geometric area of the electrode tested was F = 0.785 cm². Constant temperature of the electrolyte was maintained at 25°C by a thermostat. Current potential plots recorded are shown in figure 5.

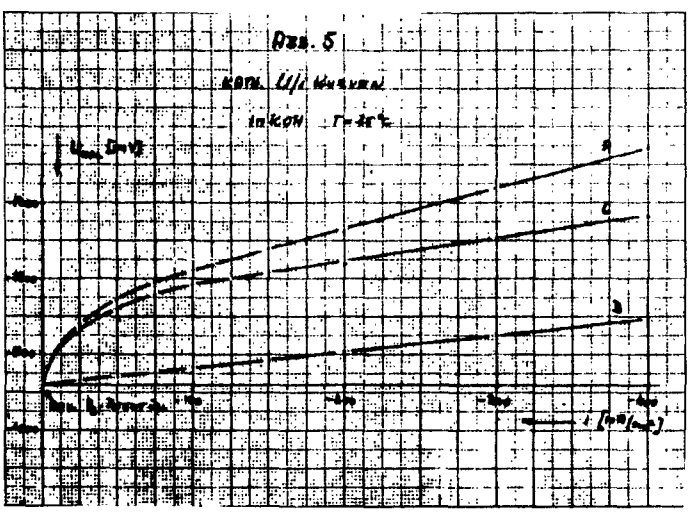

Figure 5

In order to get troubles roughly eliminated, caused by the ohmic drop within the electrolyte, the distance between the electrode surface and the Haber-Luggin capillary used was changed for 4 mm. Before and after shifting the capillary the current-potential curves were recorded. Provided a linear ohmic drop of the potential, the resistance of the electrolyte per mm can be calculated from the

potential difference obtained for constant current density. The current voltage could be obtained if the capillary was brought very close to the surface. Using this curve a plot of log $|i|$ vs. potential yields a divergence of the Tafel slope b = -120 mV, which, however, is only due to the higher current densities applied. At small current densities b = -30 mV has been proved. Plotting of this divergence in mV vs. applied current densities i results in a straight line (of. curve B of Fig. 5), which would be due to an ohmic drop caused by an actual 1.3 mm distance of the capillary. Because of the inhomogeneous surface of sintered electrodes an exact evaluation of the distance is hardly possible. So this estimation may be of use. In the clear distance the diameter of the capillary was about 0.5 mm. The capillary could not be pressed tightly to the electrode in order to avoid damage of the sintered surface. The effective surface, besides is scarcely represented only by the external peaks of the sintered material, since inner pores also support electrochemical reactions. So this correction based on an actual capillary distance of 1.3 mm seems to be very probable. Correction performed as described above provides curve C of figure 5. Figure 6 shows a plot of log i vs. potential U.

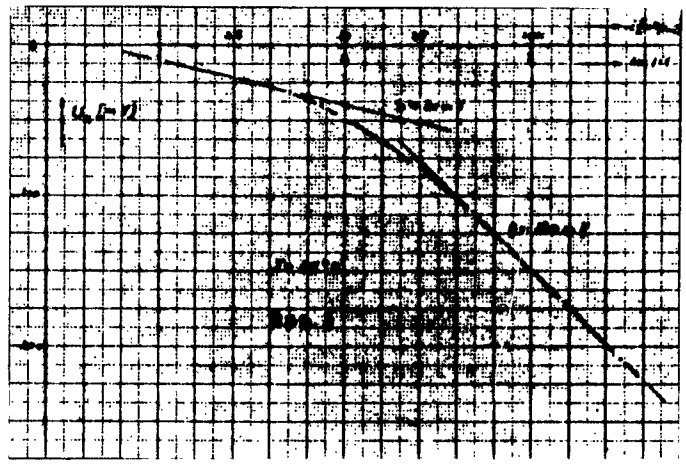

Figure 6

The two Tafel lines resulting correspond very well to the theory contained in the preceding chapter. The cathodic hydrogen overpotential of sintered, highly activated nickel electrodes is caused, therefore, by a slow recombination reaction (b = -30 mV) and by the rate of the change transfer (b = -120 mV). Using alkaline solutions similar results have been obtained for platinated platinum by

K.Dürkes [17] and for smooth platinum electrodes by Schuldiner [18] and Clamroth-Breiter [16].

5.3 Anodic Hydrogen Over-Potential

According to our experience there is a difference in the circuits of less or more activated electrodes of porous nickel electrodes. As described later on, highly activated nickel electrodes behave like platinated platinum electrodes, carefully activated and polarized in alkaline solutions. The experimental results of our impedance measurements can be interpreted in accordance with the theories of Dolin-Ershler [2] and Warburg-Breiter [3,4], derived for smooth platinum electrodes.

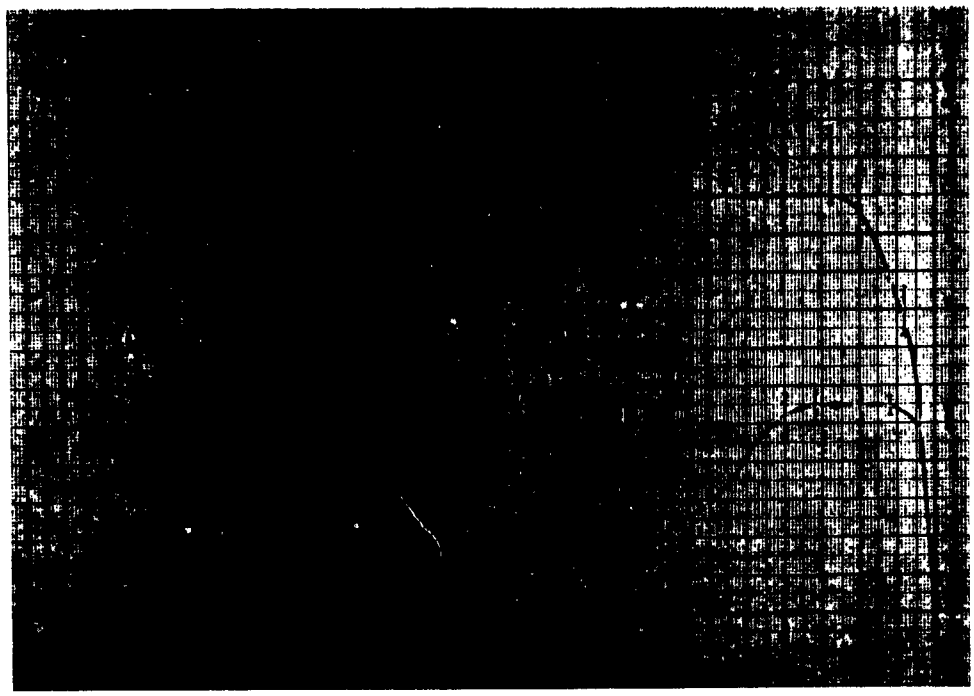

Figure 7

Figure 7 shows a typical current-voltage curve recorded at reduced temperature on a highly activated porous nickel electrode under stationary condition with an all-electronic potentiostat. The electrolyte 1N KOH was hydrogen stirred. The voltage U is the overpotential referred the reversible hydrogen potential obtained in the same electrolyte. i corresponds the current density. Starting from the reversible hydrogen-potential the applied voltage was raised stepwise in anodic

direction (curve A in figure 7). At approx. +50 mV the range of a limiting diffusions current is reached corresponding to the diffusion controlled anodic dissolution of hydrogen. The current densities are very much dependent on the intensity of hydrogen stirring. Coming up at +200 mV current densities drop with increasing voltage. From approx. +300 mV they get completely independent of stirring. Constant values of about 0.065 mA/cm^2 are obtained till reaching +650 mV. It can be assumed that the current drop is due to chemisorbed oxygen [4]. Measurements were continued up to +700 mV (not contained in fig. 7) Raising the potential up to +700 mV and beyond it the current densities increase slightly and get finally 0.15 mA/cm^2 at 800 mV. Subsequently curve B was recorded by starting at 800 mV and changing theapplied voltage in the opposite direction. Down to +350 mV curve A and B are identical. At lower potentials we get now essentially reduced currents compared to curve A. Not before +100 mV there is a limitary hydrogen diffusion current, strongly dependent on the degree of stirring, yet reduced to approximately half the size recorded in curve A. From this it follows that above +300 mV oxygen is chemisorbed operating strong binding forces to the atoms of the nickel surface. Thus the electrode area is partly blocked for the dissociation reaction of molecular hydrogen.

5.4 Results of AC-Measurements on Highly Activated Porous Nickel Electrodes

In figure 8a the capacitive components C_p of the impedance are plotted against the potential U of the electrode for various frequencies of the superposed AC. The curves run over maxima at about +150 mV. Slightly increasing C_p-values below U = 0 mV are attributed to the interference of molecular hydrogen [2,4]. Rising C_p above U = +800 mV is likely due to evolution of molecular hydrogen. Between U = +500 mV and U = +700 mV the essentially reduced C_p-values remain nearly constant. In this interval of applied voltages the surface of the nickel electrode causes, as already described, a certain irreversibility of the process (Kammermeier [3] et alt.). (Figure 8a). This results in an enlarged faradaic impedance $\mathcal{R}$, which causes neary the total A.C. to flow over the capacity C_D of the double layer connected in parallel. The values of the capacity C_p measured for this intervall of applied potentials, therefore, correspond virtually to the capacity of the double layer. Because of the high value of the dipole moment we assume the chemisorbed oxygen to interfere with the double layer. (6) (8). In figure 8b C_p-values of several steady state potential between +100 and +200 mV do not take a horizontal course for low frequencies, thus diverging from the theory of Dolin-Ershler.

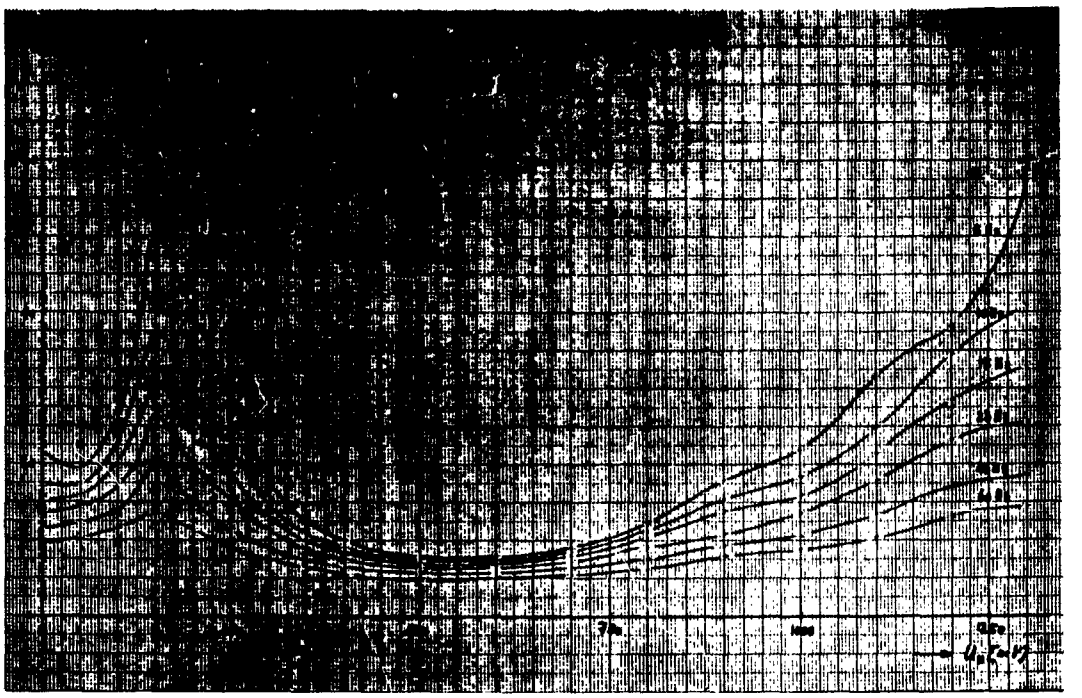

Figure 8a

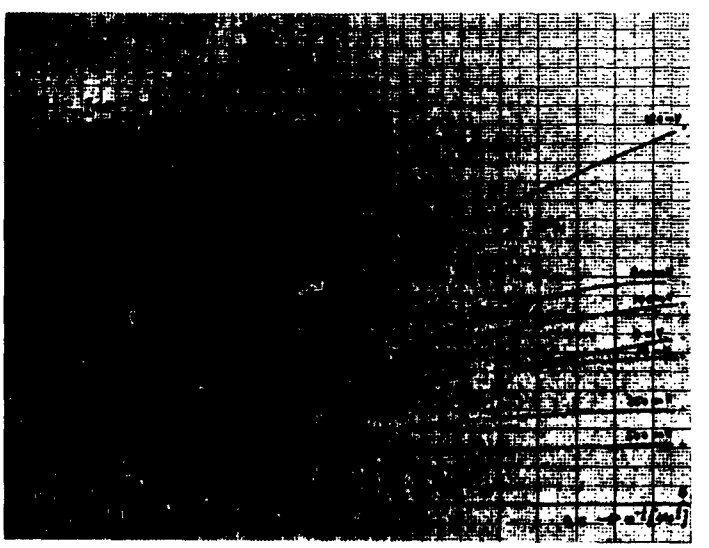

Figure 8b

Clearly, however, the C_p-values tend to a limit. The amounts of adsorbed hydrogen atoms can be determinded by extrapolating the C_p-curves to $\omega = 0$. So after subtracting the capacity C_D of the double layer we can get the so-called pseudo-capacity C_2 of the adsorbed layer. The $C_p - \omega^{-1/2}$-curves for the respective potentials between 0 and +50 mV are straight lines for the range of small frequencies, which provide the $C_s + C_D$-values after extrapolating to the frequenc $\omega = \infty$ according to the theories of Warburg and Breiter. The amounts C_p for the potentials between U = +350 mV and U = 700 mV are essentially smaller than for voltages below this region. Besides, there is no dependence on frequency as already described. These C_ps are due to the capacity C_D of the double layer and are used for the correction of the C_ps.

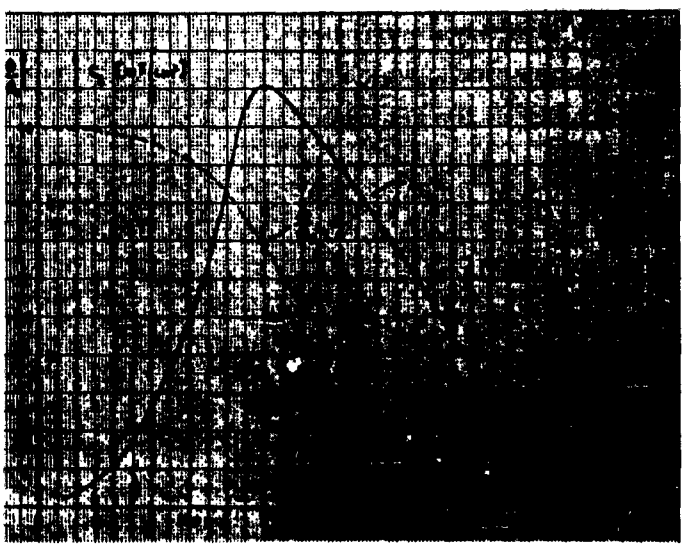

Figure 8c

In figure 8c the C_2-values evaluated as described and $\frac{\Theta}{\Theta_o}$ the standarized part of the electrode surface covered by adsorbed hydrogen, which was calculated by a stepwise integration, are plotted versus voltage U. Coming to the zero-potential the amounts of adsorbed hydrogen tend to a limit corresponding to a completed adsorption layer. This value was taken to standarize the $\frac{\Theta}{\Theta_o}$-curve.

5.5 Results of AC-Measurements on Less Activated Porous Nickel Electrodes

Porous nickel electrodes were used which remained in the open air for about 24 hours. There was no anodic pretreatment, but only a 1 hour cathodic charging with hydrogen in 1N KOH. Nevertheless these electrodes built up the reversible hydrogen potential if hydrogen bubbling was provided. The experimental results could not be interpreted with the aid of the theories of Dolin-Ershler and of Warburg-Breiter.

After converting the impedances in terms of a connection in series plotting of R_s and $\frac{1}{\omega C_s}$ against $\omega^{-1/2}$ gives parallel lines if a diffusion process alone determines the impedance. According to theoretical calculations the $\frac{1}{\omega C_s}$ -curve runs through origin, the R_s-curve is situated over it. Our investigations on less activated electrodes prove not only diffusion but also a strong influence of adsorption capacities. There is likely a surface diffusion involving hydrogen of the inner regions of the sintered electrode which interferes very much with the determination of the pseudocapacity of the adsorbed hydrogen.

Conceiving the impedance as a connection in series (of Warburg [3] et alt. [19,14]) the plots of the real and the imaginary terms versus $\omega^{-1/2}$ yield parallel lines only for higher frequencies. The straight line corresponding to the imaginary component $\frac{1}{\omega C_s}$ passes through origin (of. figure 9). At low frequencies, e.g. 5 and 10 cps the respective curves are bent due to the influence of adsorbed hydrogen on the impedance of the interface. Our results on less activated nickel electrodes are very similar to those obtained for Raney-nickel by Justi and co-workers [20]. According to this paper, however, hydrogen diffusion originates largely from the hydrogen atmosphere behind the electrode.

The C_p-U plot for 5 cps shows a curve similar to that represented in figure 8a. The values, however, are reduced to almost a half, likely caused by chemisorption of oxygen or electrode poisons, which lower the highly effective catalytic action of the surface for splitting up molecular hydrogen. The values of the double layer capacity equal very well those obtained on highly activated porous nickel electrodes.

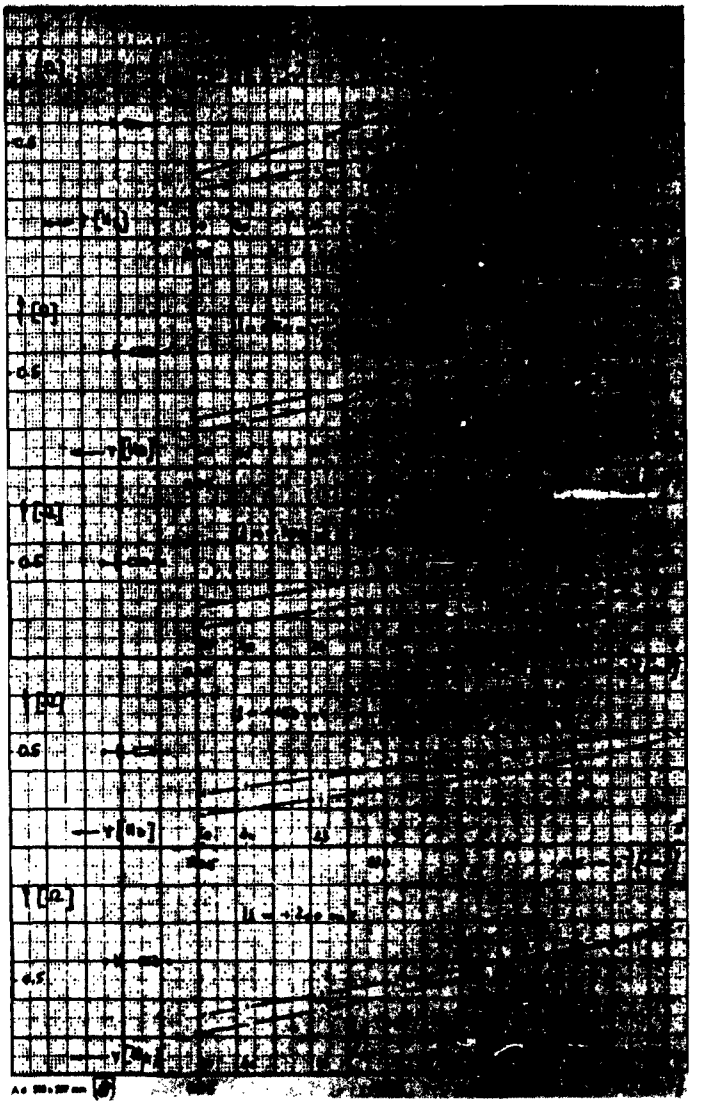

Figure 9

6. Steady-State and Impedance Measurements of the Interface Between Porous Nickel Electrodes in 1N KOH Using Various Additives as Inhibitors

Measurements of c-v-curves using the potentiostatic technique and analyses of electrode impedances were performed to study inhibition effects of various alcohols and their oxydized products. The catalytic action of the porous nickel electrodes provides in part hydrogen supply by these organic compounds. Methanol, aethanol, n-butanol, iso-butanol, glycol and glycerin were used as

additives to 1N KOH. In general, data of impedance measurements were obtained for 0.25 M alcohol + 1M KOH. The current voltage curves have been recorded in 1M alcohol + 2M KOH.

The test vessel used was similar to the previously described one. The reference electrode, however, was situated in a second compartment filled with purified KOH, which was hydrogen stirred. Bridging was done by a capillary of the Haber-Luggin type, which was drawn close to the surface of the nickel test electrode. The composed electrolytes investigated had been stirred with highly purified introgen.

We could prove an intense inhibition of hydrogen involving reactions by n-butanol and iso-butanol. Plots of the anodic current-voltage curves recorded by the potentiostatic method are shown in fig. 10.

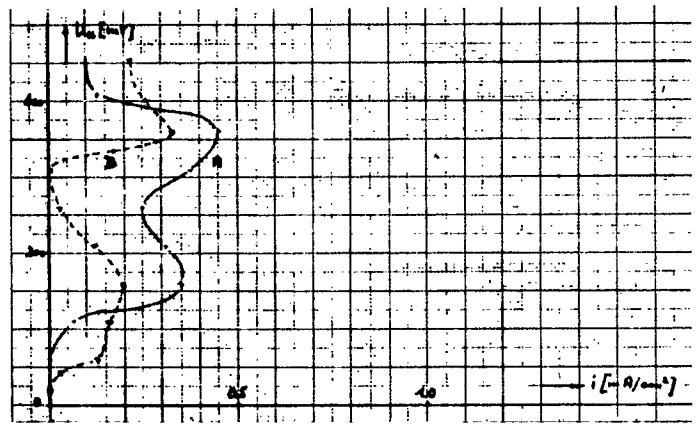

Figure 10

(Curve A responds to butanol, curve B to iso-butanol). It is indicated that these two alcohols are dehydrogenated only to a very low extent.

There is also an increased over-potential of the hydrogen evolution. E.g. cathodic charging a highly activated nickel sinter electrode with 100 mA/cm^2 in pure 1N KOH and 1N KOH with n-butanol or isobutanol as an additive results in a 500 mV difference of the overpotentials.

Additives of glycol or glycerin yield cathodic current voltage curves according to the plot of figure 11.

Figure 11

For small cathodic current densities there is hardly any influence concerning hydrogen evolution. Proceeding to a range between -250 and -400 mV vs. the reversible hydrogen potential the current suddenly begins to oscillate. If a voltage of the range mentioned above is applied only for about 1 minute, a steady-state current density finally results, which is decreased to about one hundredths the value started from. Hydrogen evolution is nearly blocked on account of a complete inhibition. Proceeding to move cathodic potential these residual current remain constant. Between 600 and 700 mV the immediate raising of inhibition is announced by small oscillations of the current density. The resulting value hardly differs from that obtained if the same potential is applied to our electrode in pure 1N KOH. The effect described we have got for both additives, glycerin and glycol. The potentials due to the beginning or raising of inhibition shifted within 150 mV. Data as compiled in the plot of figure 11 were recorded for a solution containing 120 cm^3 glycerine, 28 g KOH, and 380 g H_2O.

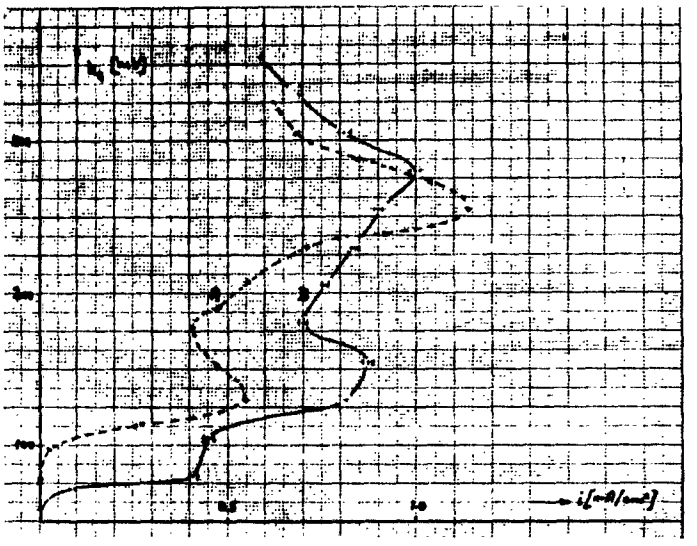

Figure 12

The respective anodic current potential curves for glycerin (curve A) and glycol (curve B) additives to 1N KOH for a positive range of potentials is shown in figure 12. The dependence of C_p in U for the same range of the potential scale is shown in the figures 13 and 14. These plots have been recorded by using the AC -method. Comparing the current-potential curves to those of figure 10 proves a far better dehydrogenation of the electrode for glycerine and glycol than for n-butanol and iso-butanol. Small positive over-voltages already provide a strong increase of anodic current densities due to electrochemical dehydrogenation. As to be seen in figure 13 in case of glycerin additives, the porous nickel electrode gets inhibited by an oxydized compound if a potential of approximately +150 mV is exceeded. For comparison these is also a dotted plot of a C_p-U-curve, which was recorded on the same electrode immersed in a hydrogen stirred solution of pure 1N KOH.

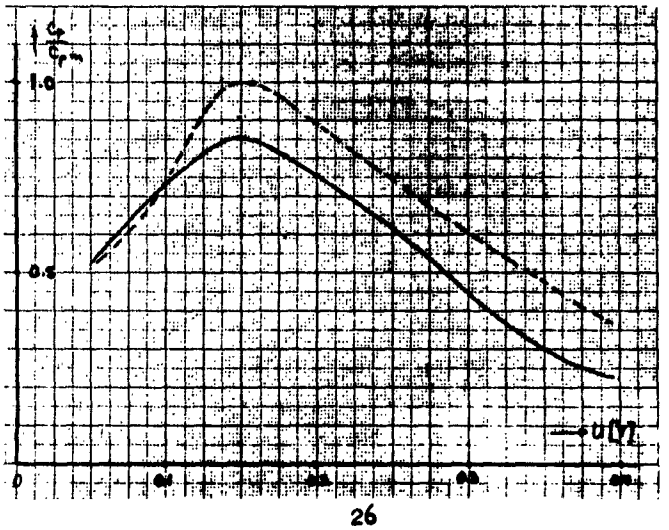

Figure 13

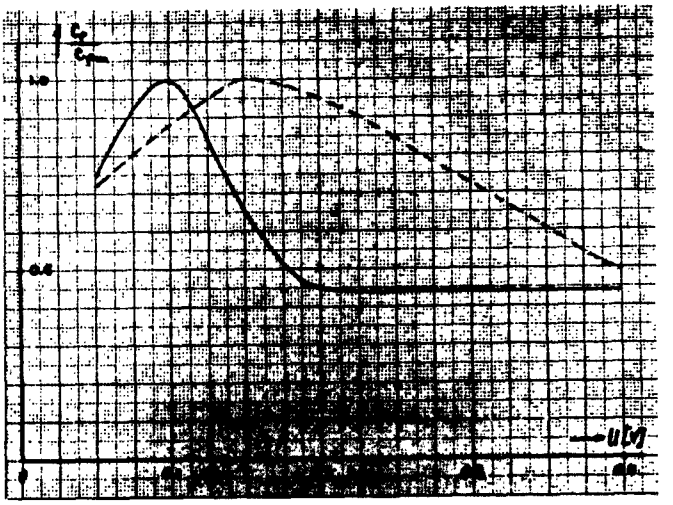

Figure 14

Up to this potential the two C_p-U-curves run almost indentically, as shown in figure 12, the beginning of inhibitive action coincides with the maximum of the current density at +150 mV. This gets even more obvious, if additives of glycol are investigated. Fig. 14 illustrated the beginning of inhibition at 100 mV and, finally, exceeding +200 mV, the blocking of electrode processes by the products of dehydrogenation. A similar effect is reported by Breiter [21] who studied phenomena of adsorption on platinated platinum using amylalcohol as an additive to alkaline solutions. Applying more positive potentials yields smaller C_p-values, which are attributed to the double layer capacity, as already described. Exceeding about +100 mV the anodic current densities are supported by another electrochemical process, which comes to a close at a potential of about +200 mV (curve B of figure 12). Products generated by oxydation processes like this will likely cause inhibition of the nickel surface.

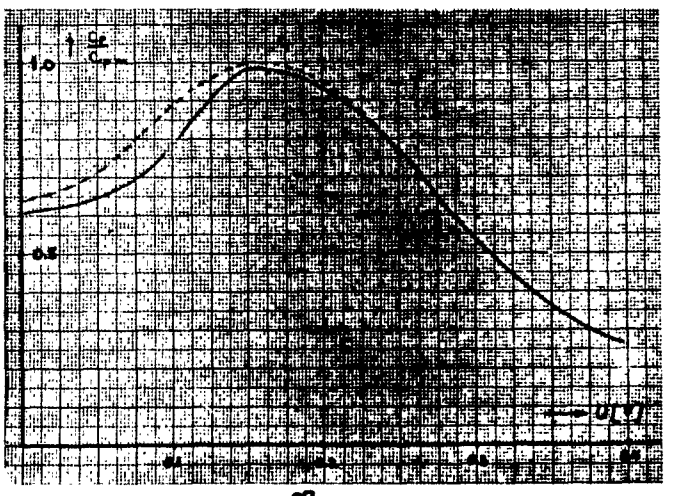

Figure 15

There is little or no inhibition influence on the activity of porous nickel electrodes if methanol or aethanol is employed as an additive to 1M KOH. The C_p-U-curves of figure 15, recorded for hydrogen bubbled KOH and for nitrogen KOH with an additive of aethanol show hardly any difference. The respective AC-measurements prove amounts of adsorbed hydrogen, which are in a good agreement in either case. In comparison to investigations in KOH-electrolytes the cathalytic action of our electrodes is lowered to a certain degree in the presence of methanol additives. (cf. figure 16).

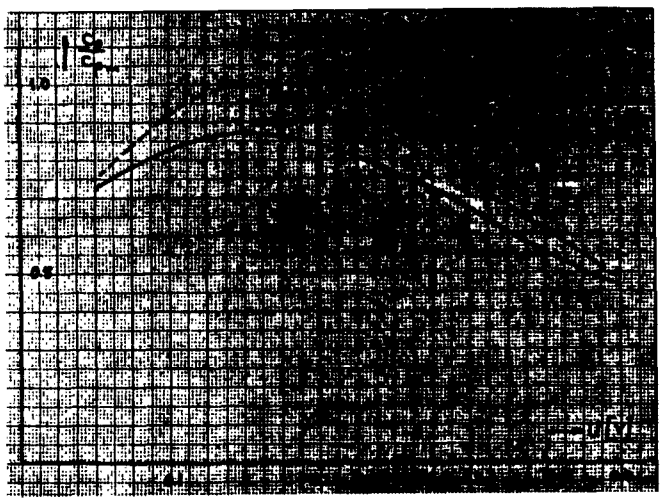

Figure 16

The general shape of the curve, however, is preserved. The respective current potential curves for methanol and aethanol additives recorded with the aid of a potentiostatic device are shown in figure 17. Though nitrogen bubbled out porous nickel electrodes build up a reversible hydrogen potential if aethanol is present (cf. curve A of figure 17).

Already slightly increased positive potentials cause a sharp rise of anodic current densities. Besides, aethanol does not inflect cathodic hydrogen evolutions. Also thus indicating a reversible build-up of open-circuit potential. Between +25 and 100 mV a diffusion-controlled limiting current is yielded, which is highly dependent on the degree of stirring. Diffusion transported aethanol is likely oxydized according to primary step of reaction.

Proceeding to more positive potentials causes increased current densities, having a maximum value at +350 mV. This is a result of a further dehydrogenation of aethanol. The decrease of currents beyond this potential is due to chemisorbed

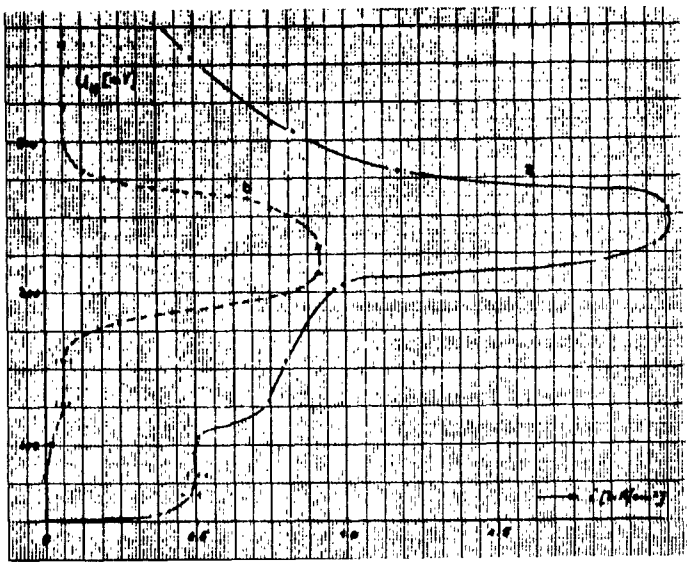

Figure 17

oxygen. Products of dehydrogenation shall be analyzed in a further research work. Dehydrogenation of methanol demands essentially increased over-potentials (cf. curve B of figure 17). There is no reversible hydrogen potential. Oxydative processes are yielded not before applying +100 mV. The respective anodic currents up to +250 mV indicate a limiting diffusion process. Applying more positive potentials provides a shape of the current-voltage-curve similar to that obtained for aethanol additives. The gross reactions, however, proceed only to a lower extent.

List of References for Part I

1. D.C.Grahame, I.Electrochem.Soc. 99, 370 (1952)
2. P.Dolin B.Ershler, Acta Physicochim. USSR 13; 747 (1940)
3. M.Breiter, H.Kammermeier u. C.A.Knorr, Z.Elektrochem. 60, 37 (1956)
4. E.Warburg, Ann.Physik 6, 125 (1901)
5. Knorr und Will, Z.Elektrochem. 64, 258 (1960)
6. Breiter und Böld, Z.Elektrochemie 64, 897 (1960)
7. Breiter und Kennel, Z.Elektrochemie 64, 1180 (1960)
8. A.Eucken und B.Wablus, Z.Elektrochem. 55, 114 (1951)
9. A.Slygin, B.Ershler, Acta Physicochem. USSR 11, 45 (1939)
10. K.Franke, M.Breiter, C.A.Knorr, Z.Elektrochem. 63, 226 (1959)
11. K.F.Bonhoeffer, H.physik.Chem. A 113, 193 (1924)
12. I.Tafel, Z.physik.Chem. 50, 641 (1905)
13. I.Heyrowsky, Recueil Trav.chim.Pays-Bas 46, 582 (1927)
14. H.Gerischer Z.Physik. Chem. 198, 286 (1951)
    201, 55 (1952)
    N.F. 1, 278 (1954)
    N.F. 8, 137 (1956)
15. L.P.Hammet, I.Amer.chem.Soc. 46, 7 (1924)
16. Clamroth and Breiter
17. K.Dürkes, Z.Elektrochem. 55, 280 (1951)
18. S.Schuldiner, I.electrochem.Soc. 99, 488 (1952)
19. B.Ershler u. M.Proskurmin, Acta Physicochim. USSR 11, 45 (1939)
20. E.Justi, M.Pilkuhn, W.Scheibe u. A.Winsel Abh.Akad. d.Wiss. Mainz 8 (1959)
21. M.Breiter, J.Electrochem.Soc. 109, 42 (1962)

Part II

1. Summary

The applicability of the potentiostatic method of applying triangular voltages was examined on bright nickel electrodes. The electrolytes 8N H_2SO_4 and 1N KOH in general were stirred with purified nitrogen.

In 8N H_2SO_4 the Coulomb charges for transforming the surface layers cannot be evaluated in term of quantity because of delayed changes of the passivating layers, and because of the large anodic currents corresponding to the corrosive dissolution of nickel. The removal of the primary layer is less restrained. The reduction of the passivating film is delayed till reaching the range of hydrogen evolution.

For nickel electrodes in 1N NaOH the instationary change of a surface layer can be evaluated by means of multi-cyclical measurements. This is due to the blocked corrosion in alkaline solutions.

Superposing a second triangular wave on a triangular carrier sweep provides measurements on highly porous nickel electrodes.

The applicability of the potentiostatic method of triangular voltages to show the influence of inhibitors by applying the principle of Wagner-Traut was examined. The change of the corrosions potential ε_{korr} and the current densities i_{korr} as a function of the concentration of added inhibitors depends on the shape of the partial-c-V-curve of the cathodic evolution of hydrogen and the anodic dissolution of the metal which depends on the surface quality of the test electrode. The partial curves in the surrounding of the corrosion potential can be determined by a graphical extrapolation of the measured entire c-V-curves at higher polarisation of the test electrodes by external currents if the test system would not be disturbed by the polarisation. The supposition is fulfilled by polarizing the electrode with the instationary method of triangular waves which is shown by the independence of ε_{korr} and i_{korr} from the different rates of potential sweep. Measurements were made at nickel and carbonyl-iron electrodes in 8N H_2SO_4.

2. The Method of Applying Triangular Waves to an Electrode

The evaluation of the kinetics of electrochemical reaction is implied by a profound knowledge of the phenomena of adsorption. Statements of this problems are often

provided by using instationary techniques [1-12], like the potentiostatic method of applying triangular voltage sweeps between the test electrode and the reference electrode, given for the first time by F.G.Will [12-13].

The voltage is increased and subsequently decreased proportionally with time ("triangular voltage"). The period of a cycle can be varied between 10^{-3} seconds and 10 minutes. Also the amplitudes of the triangular pulses are variable. A simple potentiometer device provides adjustment of a suitable starting potential. The applied triangular voltage is connected to the horizontal deflection system of a Tektronix 502 Dual-Beam Oscilloscope, which serves as a two channel X-Y-recorder. The respective currents flowing between the test electrode and the counter electrode cause voltages across a standard resistor, which are applied to the vertical deflection system of the oscilloscope. The resulting current potential curves are quasi-stationary if low rates of the sweep are employed. When increasing the rates continuously there is a continuous transition from the stationary to the instationary state, so that the processes of charge transfer become more and more prevailing against the transport processes. If there is a speedy adjustment of the adsorption equilibrium compared to the rate of the voltage sweep, i.e. if the stationary equilibrium of adsorption, which is dependent on the potential of the electrode, remains adjusted, the quantities of charge used up can be obtained directly as a function of potential by means of a stepwise graphic integration of the photographic current potential curves or current-time-curves respectively. On these preconditions any cycle can be used for evaluating the charges, otherwise the anodic and cathodic sections of a sequence of cycles must be integrated on the whole.

3. Bright Nickel Electrodes in 8N H_2SO_4

3.1 Open-circuit Potential

A delay of the build up of the corrosion potential was found for bright nickel electrodes in 8N H_2SO_4, which was vigorously stirred, with highly purified nitrogen. The electrodes were cleaned with concentrated $HClO_4$, thoroughly rinsed with bi-distilled water, and subsequently transferred to the test vessel. At first a potential U_h = -67 mV vs. a hydrogen-bubbled plate of platinated platinum was obtained. The values of potential, however, increased with time; e.G. after 3 hours U_h = -40 mV resulted. About 8 hours past U_h = -27 mV a steady-state corrosion potential could be obtained.

3.2 Stationary Current Potential Curves [14-15]

3.2.1 Experimental

The test vessel already described was used, the c-V-curves were recorded with the aid of an electronic potentiostat, which was delivered by Bank Ltd., Göttingen, (Wenking device). Proceeding to more positive potentials in steps of 50 mV, voltages of the range between U_h = -350 mV and U_h = +1550 mV were applied to the test electrode. By means of a simple potentiometer device the potentials could be altered. The respective potentials were maintained for 20 minutes. The resulting current densities are assumed to be stationary except those recorded for the potentials between +100 mV and +300 mV. The electrode potentials was controlled vs. reference potentials with the aid of a Knick-amplifier (Knick Ltd. Berlin, type 62 Nr. 2026), d-c was measured with a micro-Am-meter of Siemens and Halske Ltd. Ni(II)-ions, e.g.formed during corrosion, did not influence the shape of the c-V-curve.

3.2.2 Discussion

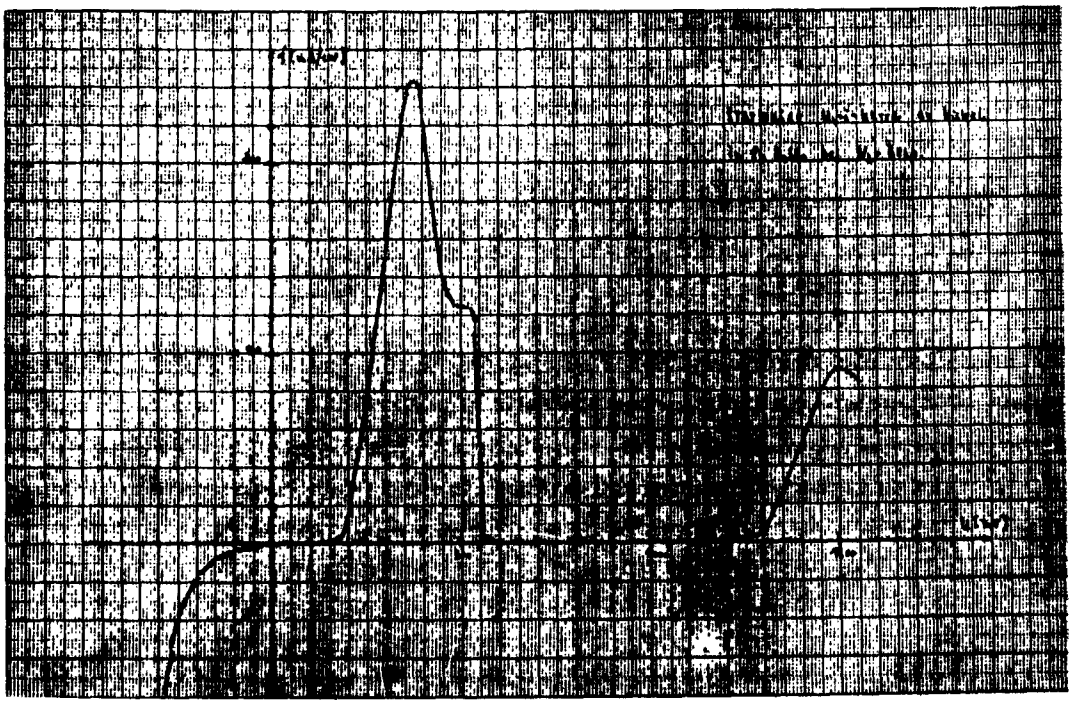

Figure 18

There is only a slow open-circuit corrosion of nickel. As shown in figure 18 the current potential curve can be divided into six succeeding ranges, which are characterized by different stationary material states of the nickel surface. Below the open-circuit potential cathodic hydrogen evolution occurs to an increasing extent. Above this potential nickel seems at first to be activated and dissolves anodically in its divalent state. Exceeding U_h = +350 mV the oxydation of nickel gets more and more controlled by a surface layer. The current densities decrease to almost half of the maximum value obtained for U_h = +380 mV. Not till U_h = +560 mV do we get the nickel surface passivated by a change of the layer mentioned above. The potential characterizing the formation of a second layer may be called the Flade potential of nickel. It can be produced within 3 mV. In the region of passivity anodic steady-state current densities amount to 1.5 mA/cm², which are strongly increased compared to those recorded on carbonyl iron electrodes. (1.4 μ A/cm² or 0.7 μ A/cm² respectively) [16-17]. According to a paper of K.J.Vetter the passivating film on nickel consists of NiO, due to the reaction

$$Ni + H_2O \rightleftharpoons NiO + 2H^+ + 2e^-$$

The increase of anodic current densities applying potentials more positive than +1200 mV results in a maximum at approx. U = +1500 mV. For this region K.J.Vetter postulates a corrosion process which involves the passivating film. The subsequent range of positive potential molecular oxygen is developed.

3.3 Instationary Current Potential Curves

3.3.1 Experimental

The test electrode of highly purified nickel was immersed in 8N H_2SO_4, which was saturated with nitrogen by vigorous gas-stirring. The electrode potentials U_h are referred to a hydrogen-bubbled plate of platinated platinum being in the same electrolyte. Like the steady-state investigations also the instationary measurements yield significant waves, which indicate the formation of surface layers.

At first the general shape of the curves obtained may be discribed:

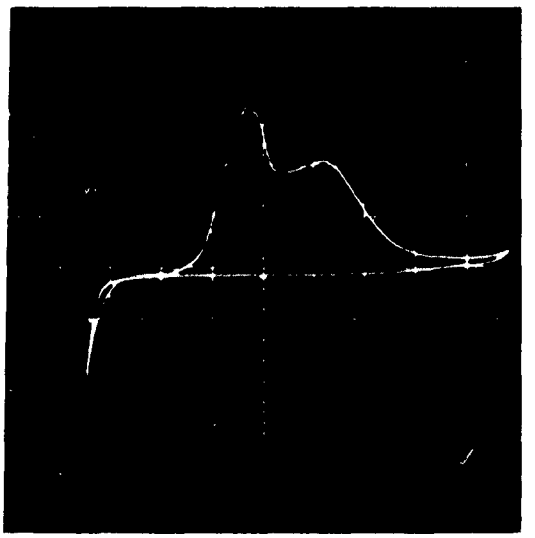

Figure 19

Limits of triangular pulse	-350 mV, +1400 mV
Rate of potential sweep	0.5 volt p.s.
Scale unit of the ordinate	60 mA
Scale unit of the abscissa	200 mV

The current voltage curve shown in figure 19 was recorded by applying to the electrode a potentiostatic potential sweep running between U = -350 mV and U = +400 mV. The rate of potential shift employed was 1 V p.s. (scale unit for the ordinate 60 mA/cm², for the abscissa 200 mV.) Comparing the anodic sweep of figure 19 to the plot of figure 18 shows that the general shape of the curve is quite the same. Only the plateau situated under stationary conditions at U_h = +560 mV has changed into a flat maximum and the strong decrease of current densities due to passivation has shifted a little bit. The cathodic sweep yields only small cathodic currents which increase below U_h = -200 mV according to hydrogen evolution.

The shape of the cycles recorded with the oscilloscope is dependent on the rate of the potential shift and the limiting potentials of the triangular voltage sweep.

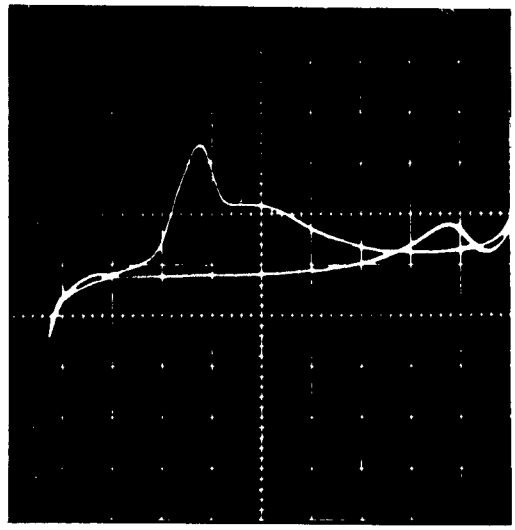

Figure 20

Limits of triangular pulse	-350 mV, +1600 mV
Rate of potential sweep	1 volt p.s.
Scale unit of the ordinate	60 mA
Scale unit of the abscissa	200 mV

Figure 20 shows a photograph taken on applying triangular sweep between U_h = -350 mV and U_h = +1600 mV. The sweep rate was again 1 V p.s. Due to a more positive limiting potential of the triangular voltage pulse the cathodic sweep provides a maximum of anodic currents at U_h = +1500 mV which likely corresponds to the maximum of corrosion found by K.J.Vetter on stationary measurements. Applying a constant sweep rate of 1 V p.s. the cathodic limit of the triangular pulse was fixed whereas the anodic limit was shifted from U_h = +1600 mV to U_h = +300 mV in steps of 50 mV.

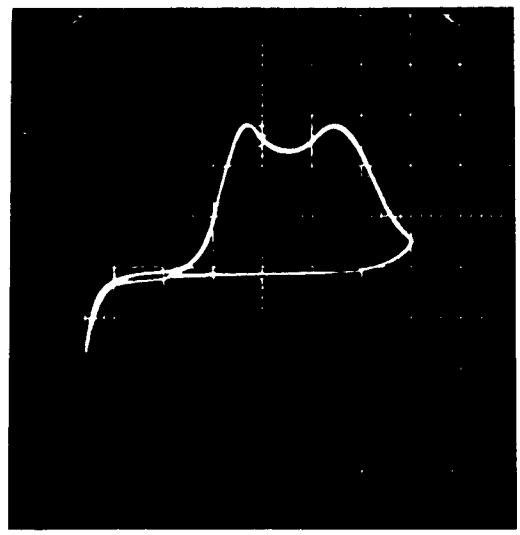

Figure 21

Limits of triangular pulse	-350 mV, +1000 mV
Rate of potential sweep	1 volt p.s.
Scale unit of the ordinate	70 mA
Scale unit of the abscissa	200 mV

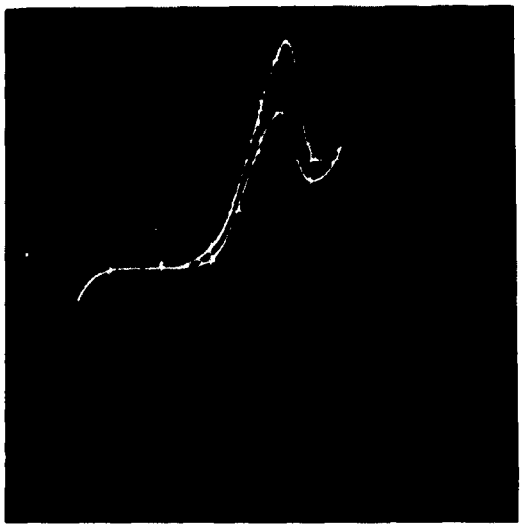

Figure 22

Limits of triangular pulse	-350 mV, +700 mV
Rate of potential sweep	1 volt p.s.
Scale unit of the ordinate	140 mA
Scale unit of the abscissa	200 mV

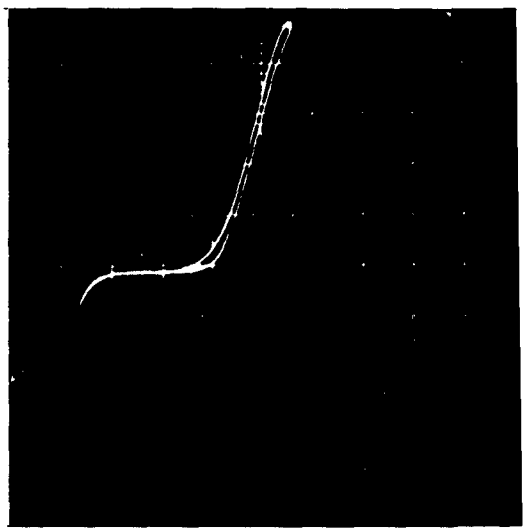

Figure 23

Limits of triangular pulse	-350 mV, +500 mV
Rate of potential sweep	1 volt p.s.
Scale unit of the ordinate	140 mA
Scale unit of the abscissa	200 mV

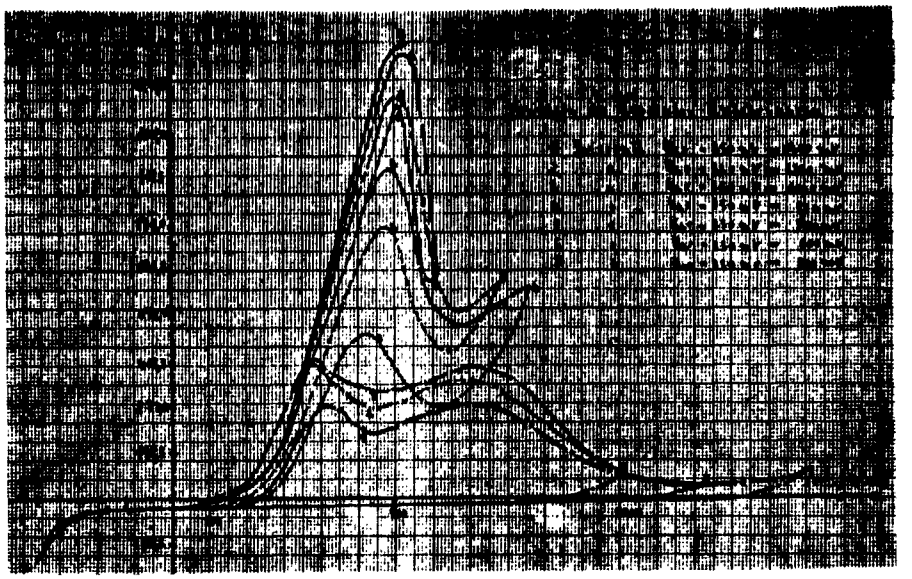

Figure 24

As shown in the photographs of the figures 21, 22, 23, and in the plot on figure 24 the respective current densities of the anodic sweep increase with shifting the potential of the anodic limit to less positive values.

In another series of investigations the triangular sweep was run to a constant anodic limit of U_h = +1400 mV. Now the cathodic limit was shifted to less negative potentials within the range between U_h = -350 mV and U_h = 0 mV.

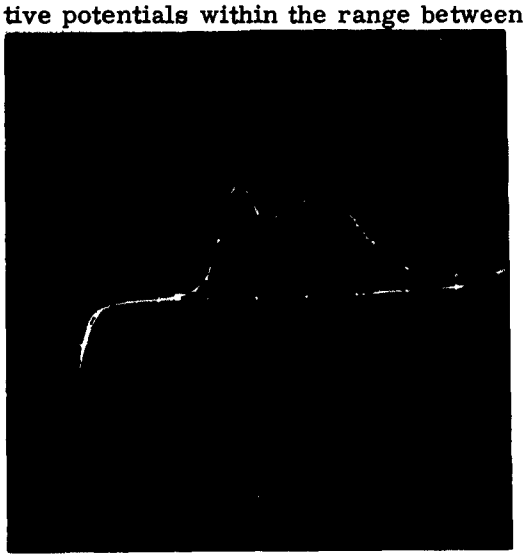

Figure 25

Limits of triangular pulse	-350 mV, +1400 mV
Rate of potential sweep	1 volt p.s.
Scale unit of the ordinate	70 mA
Scale unit of the abscissa	200 mV

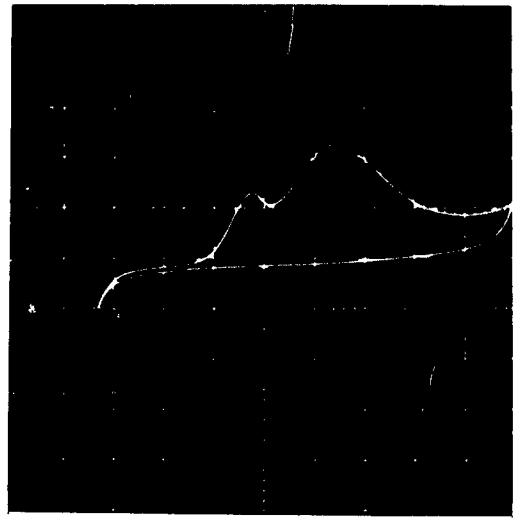

Figure 26

Limits of triangular pulse	-250 mV, +1400 mV
Rate of potential sweep	1 volt p.s.
Scale unit of the ordinate	28 mA
Scale unit of the abscissa	200 mV

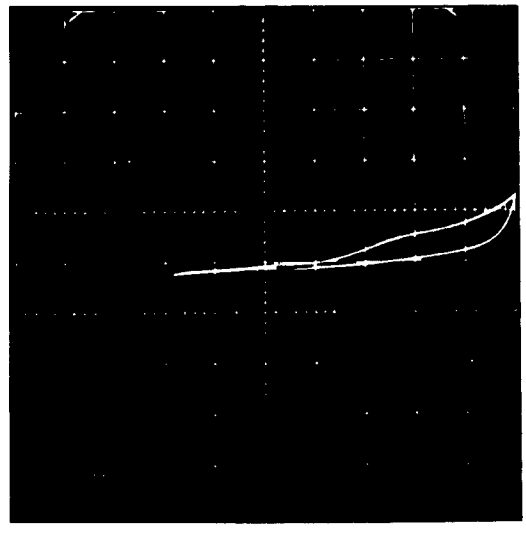

Figure 27

Limits of triangular pulse	0 mV, +1400 mV
Rate of potential sweep	1 volt p.s.
Scale unit of the ordinate	28 mA
Scale unit of the abscissa	200 mV

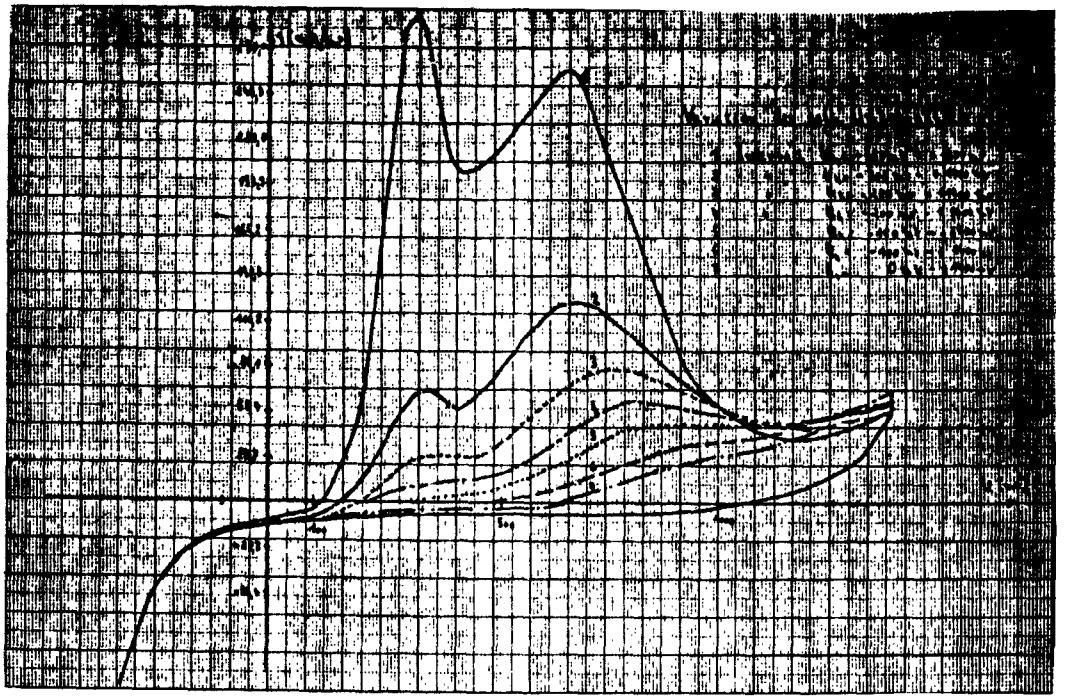

Figure 28

From this results a decrease of the anodic current densities corresponding to the anodic sweep of the triangular pulse as shown in the photographs of the figures 25, 26, 27, and the plot of figure 28. The curves recorded were not dependent on the degree of gas stirring. The same results could be obtained whether hydrogen, nitrogen, or oxygen bubbling was employed.

Besides, tests have been performed concerning the dependance of instationary current potential curves on the rate of the triangular sweep. The respective current potential curves for increasing the rate of potential change within constant range limited by U_h = -350 mV and U_h = +1400 mV are shown in the photographs of figures 29, 30, and 31 and the plot of figure 32.

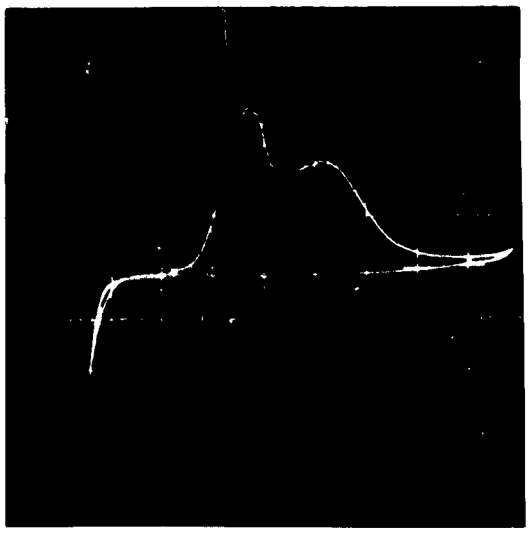

Figure 29

Limits of triangular pulse	-350 mV, +1400 mV
Rate of potential sweep	0.5 volt p.s.
Scale unit of the ordinate	60 mA
Scale unit of the abscissa	200 mV

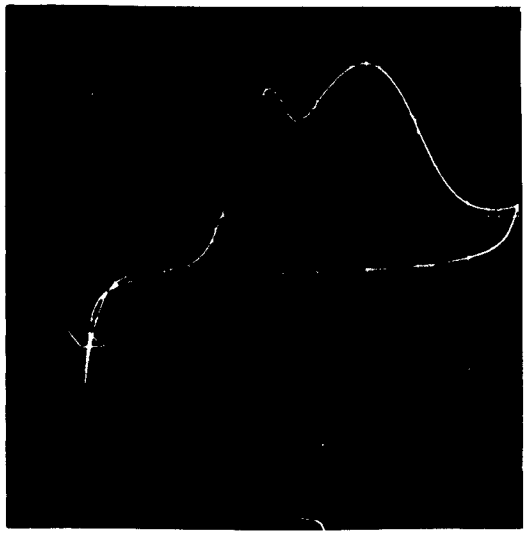

Figure 30

Limits of triangular pulse	-350 mV, +1400 mV
Rate of potential sweep	2 volt p.s.
Scale unit of the ordinate	60 mA
Scale unit of the abscissa	200 mV

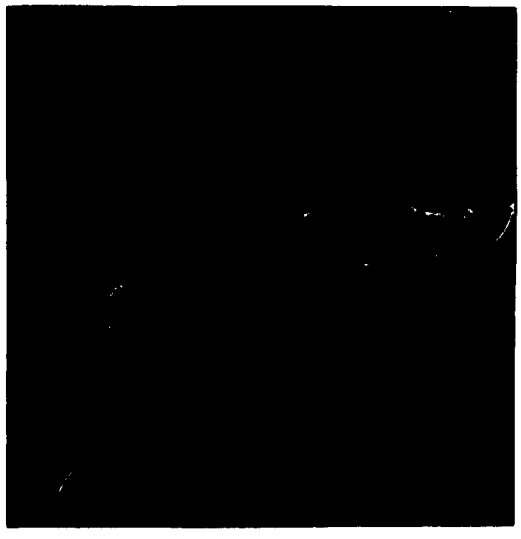

Figure 31

Limits of triangular pulse	-350 mV, +1400 mV
Rate of potential sweep	9 volt p.s.
Scale unit of the ordinate	120 mA
Scale unit of the abscissa	200 mV

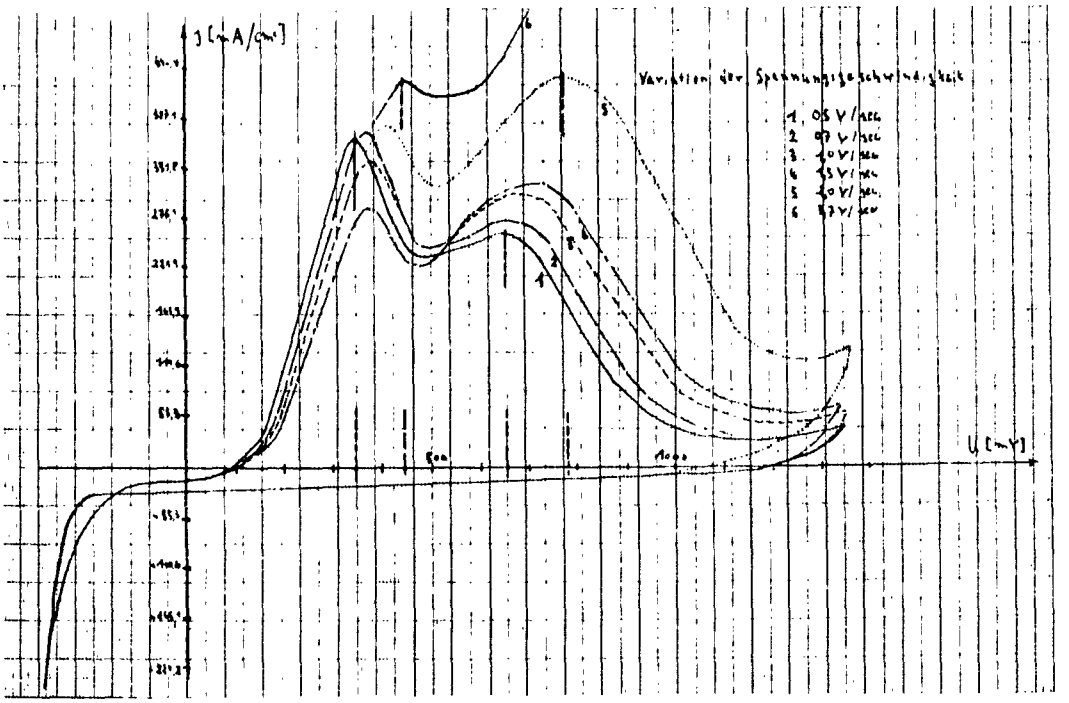

Figure 32

In general, higher rates cause larger anodic current densities during the anodic sweep of the triangular pulse. The currents corresponding to the maxima show a stronger increase. Moreover there is a shift of the potentials of the first maximum according to U_h = +380 mV for 0.5 V p.s., U_h = +450 mV for 3.7 V p.s. and concerning the second maximum according to U_h = +650 mV for 0.5 V p.s. and U_h = +780 mV for 3.7 V p.s.

3.3.2 Discussion

As already described for steady-state current potentials curves of instationary investigations prove likewise that two distinct surface layers are rate determining for the anodic dissolution process of nickel electrodes. From the variation of the anodic limiting potentials of the triangular pulse can be concluded that the reductive change of both the layers occurs on quite different rates, during the anodic sweep. The cathodic sweeps of the respective curves limited by potentials corresponding to the region of the first maximum results a less restrained removal of the primary surface layer compared to the reductive

change of the second layer being due to passivation. If the rate of the voltage sweeps is raised, the reduction of the passivating film gets more and more delayed and does not take place until increasing the cathodic over-potentials to the range of simultaneous hydrogen development. Comparing our results with those of measurements on the hydrogen adsorption on bright platinum electrodes in acid solutions, result in a remarkable irreversibility of the chemisorption layers in particular of the passivating film in case of bright nickel electrodes. Multicyclycal tests, therefore, provide phenomena due to a delay of electrode processes. For these reasons and moreover because of the large anodic currents corresponding to the corrosive dissolution of nickel, the Coulomb charges for transforming the surface layers can hardly be evaluated in terms of quantity.

4. Bright Nickel Electrodes in 1N KOH

4.1 Open Circuit Potentials

Auto-activation of the nickel electrodes in concentrated $HClO_4$ was employed. After this the electrodes were carefully rinsed with bidistilled water and finally transferred into the test solution. Nitrogen bubbled electrodes proved an open-circuit potential of U_h = +20 mV. The reversible hydrogenpotential was built up hydrogen stirring of the electrode. For oxygen bubbled test electrodes we got U_h = +1280 mV.

4.2 Quasi-Stationary Measurements

The respective potentials were applied to the electrode by an electronic potentiostat. The voltage was changed in steps of 100 mV with waiting periods of 15 minutes. In doing so steady-state conditions are considered to be obtained for the ranges of hydrogen and oxygen development.

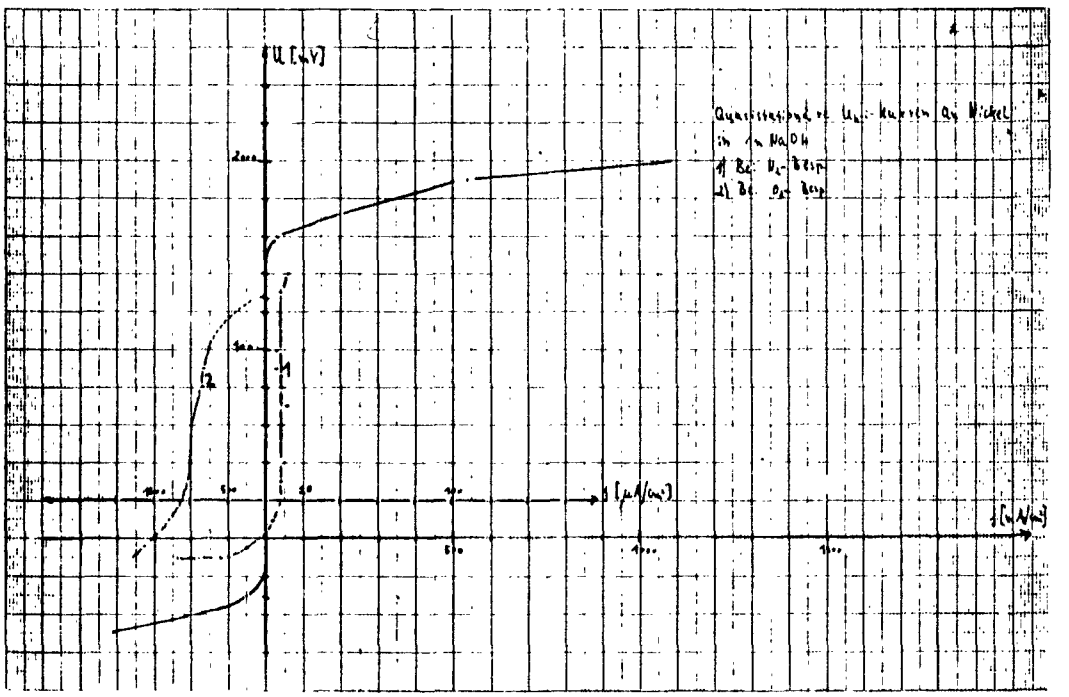

Figure 33

Figure 33 shows a current potential curve which was recorded on a nitrogen-bubbled bright nickel electrode. For the range of hydrogen development a Tafel-line can be drawn, the coefficient b of which is -119 mV. According to theoretical calculations a b-value of about -112 mV corresponds to the Vollmer-mechanism controlling hydrogen over-potentials. $b = \frac{RT}{(1-\alpha)F}$ is due to a rate determining charge transfer reaction. Applying potentials between U_h = +20 mV and U_h = +1450 mV to the nickel electrode proves small residual currents densities of about 8 $\mu A/cm^2$. Exceeding U_h = +20 mV and U_h = +1450 mV yields increasing anodic current densities corresponding to the evolution of molecular oxygen.

Bubbling the electrode with oxygen causes a cathodic limiting current of about 0.9 mA/cm^2 between U_h = +1280 mV and U_h = o mV, which is highly dependent on the degree of stirring. This is interpreted by a limiting diffusion of molecular oxygen.

4.3 Instationary Current Potential Curves

The potentiostatic method of applying triangular voltages to nickel electrodes was also used in our tests in 1N NaOH. In this electrolyte the corrosive dissolution of the metal is fairly restrained providing thus recordings of instationary changes of the coulomb charge of the respective adsorbed layers.

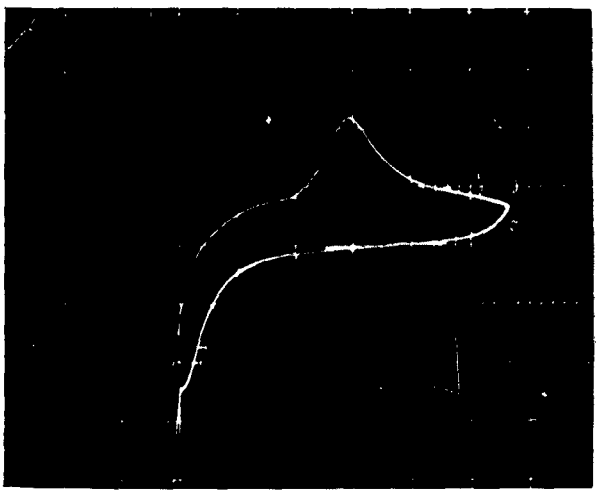

Figure 34

Limits of triangular pulse	-350 mV, +900 mV
Rate of potential sweep	1 volt p.s.
Scale unit of the ordinate	4 mA
Scale unit of the abscissa	200 mV

A series of tests may be represented by the photograph of figure 34. The triangular sweep ran all over the range between U_h = -350 mV and U_h = +900 mV with a rate of 1 V p.s. The current potential curve proves an instationary change of an adsorbed layer, which is characterized by a maximum of cathodic current densities at U_h = -200 mV, corresponding to the cathodic sweep of the triangular voltage. If the negative limiting potential is shifted to less negative values, i.e. to values beyond the region of potentials to which the currents of the cathodic wave correspond at a given rate of the sweep, also the anodic wave of the anodic sweep is wanting. From this a close connection between the reactions causing the two waves can be concluded. Increasing the rate of the triangular sweep results in a shift of the anodic wave to more positive values of the voltage applied to the electrode. This results from a restrained change of the adsorbed layer. These reactions are not influenced by a variation of the gas, used for stirring or the intensity of gas bubbling.

Also in case of our instationary measurements the coefficient of the Tafel slope b = -120 mV was preserved in a wide range of rates.

5. Application of a Modified Method of Applying Triangular Voltages to a Porous Nickel Electrode

In another series of investigations the so-called triangular-method was employed to highly porous electrodes. Figure35 shows a photograph of a current potential curve which was recorded on a highly porous nickel electrode in 1N KOH.

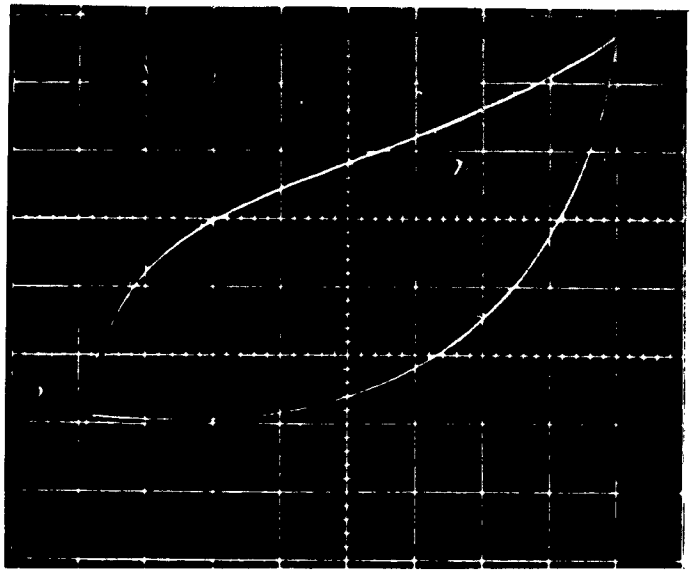

Figure 35

The amplitude of the sweep was 400 mV, starting from zero-potential with sweep rates between 1 V p.s. and 0.02 V p.s. . though prepared and described in part I of this paper the electrode which was hydrogen stirred had a slightly reduced activity because there was a difference between the nickel skeleton used. In contrast to steady-state current potential curves shown in part I of this paper, instationary measurements proved no anodic maximum due to adsorbed hydrogen. In deviation from the results obtained for instance on bright platinum or bright nickel electrodes applying the triangular method there is a steady increase of the anodic current densities till coming to the anodic limit of the triangular voltage.

This is likely caused by a delayed adjustment of the adsorptive equilibrium on the whole highly porous surface. As well known the steady state equilibrium of adsorption is a function of the potential applied. Desorption of hydrogen a comparatively speedy reaction may only occur on the peaks of the highly structured surface thus

involving perhaps the diffusion of hydrogen from the inner regions of the electrode to the said "active fraction of the surface area".

Additives of 1M aethanol or 1M methanol to 1 liter 1N KOH yield nearly the same instationary curve for the range of potentials between U_h = 0 mV and U_h = +400 mV. Nearly the same results could be obtained for porous electrodes of iron and cobalt.

To prove our interpretation the triangular method used so far was modified. Now triangular functions of smaller amplitudes and higher rates of voltage change were superposed over a triangular carrier function, data of which were similar to those used in our former experiments. The resulting function shows a subdivision into ranges of increasing and decreasing voltages involving desorption of hydrogen and diffusion to the surface, respectively adsorption and diffusion of hydrogen into the inner regions of the porous electrode. If the potential corresponding to the carrier function tends to more positive values desorption of hydrogen and diffusion to the surface prevails altogether. Assuming that desorption prevails at the potential-determining zones of the surface the superposition of small triangular amplitudes with higher frequency likely proved a more constant depth, down to which the desorptive action enters. Thus the effect of hydrogen diffusion from the inner regions of the sintered material may be determined. In consequence of this the anodic wave of desorption becomes visible at about U_h = +600 mV, as shown in the photograph of figure 36.

Figure 36

This curve was taken for an anodic limiting potential of U_h = +160 mV in order to lower the activity of the electrode and thus the current densities by an intermediate adsorption of oxygen.

6. The Method of Triangular Waves and the Principle of Wagner-Traut

In the following results a possibility to use the method of the triangular waves in the study of the effect of inhibition. The Wagner-Traut pinciple of the superposition of the partial c-V-curves of the cathodic evolution of hydrogen and the anodic dissolutation of the metal will be employed. The shape of the entire c-V-curves is additatively composed by the current densities of the two independent partial c-V-curves at the same potential. The potential in which results i = 0 is neither the open circuit potential of the reaction

$$Me \rightleftharpoons Me^{+} + Ze^{-}$$

nor the open circuit of the reaction

$$H_2 \rightleftharpoons 2\,H^{+} + 2e^{-}$$

but is between. The curent densities of the two mentioned partial c-V-curves at the corrosionspotential in which results i = 0 are opposit equal. The position of the corrosionspotential of the reaction depends on the shape of the partial c-V-curves. Therefore the position of this potential just as the shape of the partial c-V-curves depends on the quality of the surface of the test electrode, while the open circiut potentials of the partial curves are independent of the surface quality. By addition of inhibitors to the electrolyte the shape of the partial c-V-curves which represents the anodic dissolution of metal just as the partial c-V-curve which represents the cathodic evolution of hydrogen is changed. The task of a quantitative mark of the effect of the added inhibitors longs for a statement about the change of the anodic and the cathodic partial c-V-curves as a function of the concentration of the inhibitor. By higher polarisation of the electrode with an external polarisation current the measured entire c-V-curve coincides with one of the partial c-V-curves (the anodic- or the cathodic partial curve). If the system is not disturbed by the polarisation of the electrode essentially it will be possible to find out the shape of the partial c-V-curve in the surrounding of the corrosionspotential of the entire c-V-curve by an extrapolation of the measured c-V-curve at higher polarisation currents. The supposition of a non-disturbed system by polarizing the electrode is generally not fulfilled by steady-state-measurements of the entire curve because of the change of the inhibitor concentration at the surface of the electrode etc. . To avoid a perturbation

of the system by polarizing the electrode and to have a possibility to measure the entire curve as far as necessary to do the extrapolation if it is favorable to do the polarisation of the test electrode by the instationary method of the triangular waves.

6.1 Experimental

The measurements were made at nickel and carbonyl iron electrodes in 8N H_2SO_4 Auto-activation of the electrode in concentrated $HClO_4$ was employed. After this the electrodes were carefully rinsed with bi-distilled water and finally transferred into the test solution. The electrolyte was stirred with nitrogen. After obtaining stationary current densities at the stationary corrosionspotential the test electrode was polarized by the triangular waves to anodic or cathodic potentials with different rates of potential sweep. The obtained c-V-curves were photographed at the oscillograph screen. The working out of the test results shows the partial c-V-curves, the corrosionspotential and the corrosions-current-density. One obtains comparable results only by waiting to the stationary state of the current-density at the corrosionspotential before polarizing the electrode. With the nickel electrode one had to wait 3 to 5 hours, with iror electrodes $^1/_2$ to 1 hour.

To show the perturbation of the test system by polarizing the electrodes tests with different rates of potential sweeps from 0.2 V p.s. to 3 V p.s. were executed. The perturbation of the test system could be demonstrated by the change of ε_{korr} and i_{korr} with different rates of potential sweeps.

6.2 Results

I_{korr} and ε_{korr} are determined without addition of inhibitors to obtain a referring value.

Fig.37 shows the c-V-curve at an carbonyl iron electrode and the extrapolation to determine i_{korr} and ε_{korr}. An influence of the shape of the partial c-V-curves by different rates of potential sweep was not obtained and shows the applicability of the method. The measured corrosionspotential before polarizing the electrode is the same as the potential determined by the graphical extrapolation ε_{korr} was found to U_h = +160 mV i_{korr} was found to 3.05 mA/cm².

Fig.38 shows the c-V-curve at highly purified nickel electrodes under the same conditions. ε_{korr} = -28 mV and i_{korr} = 128.5 µA/cm².

Figure 37

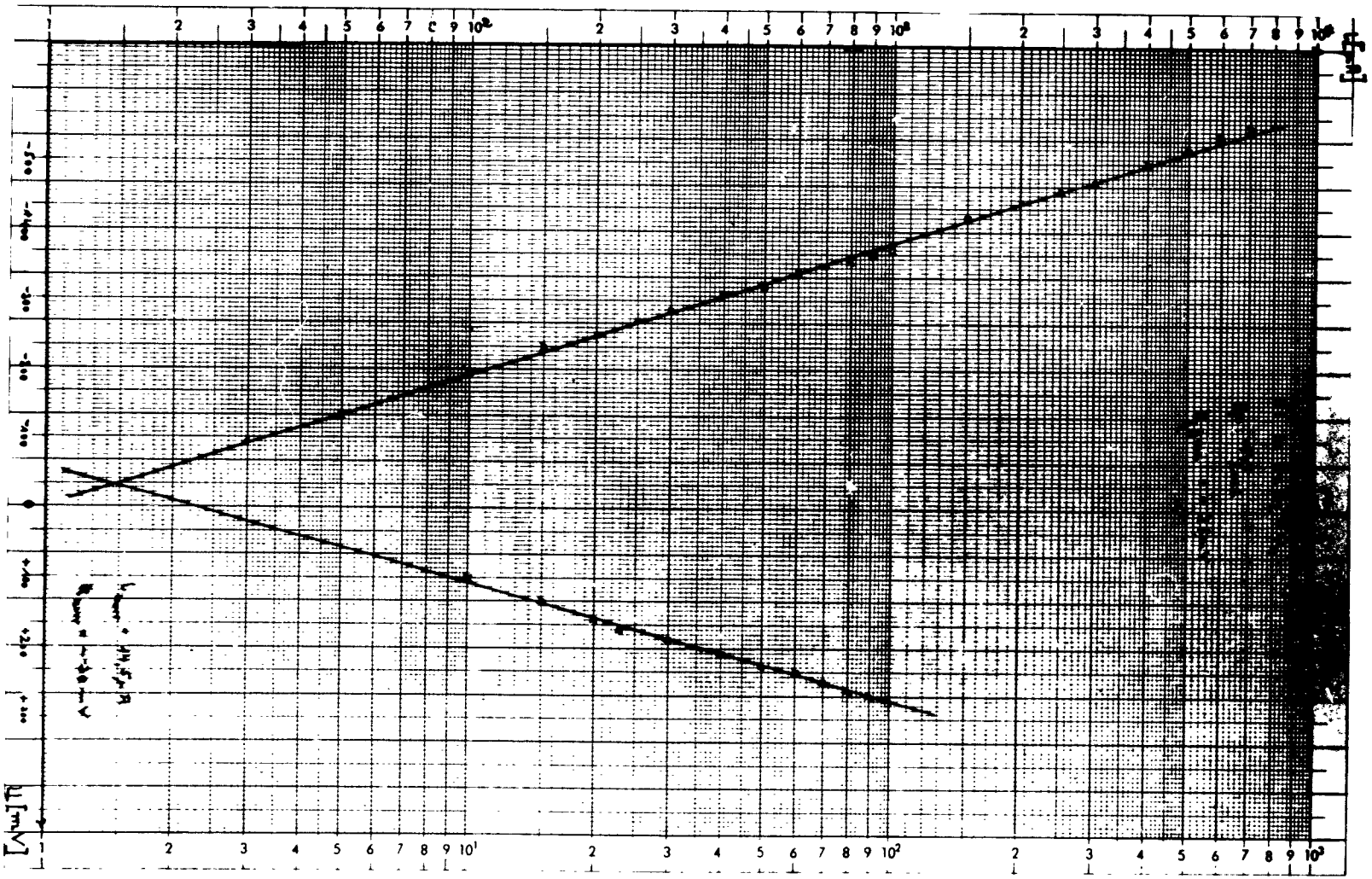

Figure 38
51

Eine Achse logar. geteilt von 1 bis 1000, Einheit 90 mm, die andere in mm

List of References for Part II

1. F.Krüger, Z.physik.Chem. 45, 1 (1902)
2. P.Dolin and B.V. Ershler, acta physicochim. USSR, 73, 747 (1949)
3. K.W.Somerton, Trans Faraday Soc. 48, 937, 951 (1952)
4. J.E.B. Randles, Discuss. Faraday Soc. 1,11 (1947)
5. R.Reichinstein, Z.Electrochem. 15, 734 (1909)
6. A.Siygin and A.Frumkin, Acta Pysicochim. USSR. 3, 791 (1930)
7. J.A.V. Buttler and G.Drever, Trans Faraday Soc. 32, 427 (1936)
8. P.Delahay, I. Amer. Soc. 73, 4944 (1951)
9. L.Gierst and A.Juliard, J.physic. Chem. 57, 701 (1953)
10. A.Hickling, Trans.Faraday.Soc. 38, 27 (1942) 41, 333 (1945)
11. P.Delahay, J.Americ. Soc. 75, 1430 (1953)
12. F.G.Will, Deutsches Patentamt, Patentanmeldung W 23858 1X/421
13. F.G.Will, Diss. TH München
14. K.J.Vetter u. K.Arnold Z.Elektrochem. 61, 1177 (1957)
15. K. Arnold u. K.J.Vetter " 64, 244 (1960)
16. G.F.Frank and K.G.Weil " 56, 814 (1952)
17. K.J. Vetter " 55, 274 (1951) 59, 27 (1955)

Aeronautical Systems Division, Dir/Materials and Processes, Metals and Ceramics Lab., Wright-Patterson AFB, Ohio.
Rpt Nr ASD-TDR-62-1067, STUDIES OF HYDROGEN AND OXYGEN EVOLUTION AND THE INFLUENCE OF ADSORBED SUBSTANCES. Final report, Mar 63, 52pp. incl. illus., 38 refs.

Unclassified Report

In this report A. C. Measurements of the interface impedance prove to be suitable for studying adsorption phenomena on porous electrodes like platinated platinum and sintered nickel material. The impedance on platinum electrodes was evaluated for 8N H_2SO_4 and 1N KOH solutions. Further investigations dealt with inhibition problems on highly activated porous nickel electrodes. Several alcohols were used as additives to 1N KOH.

The applicability of the potentiostatic method of applying triangular voltages was examined on bright nickel electrodes. The electrolytes 8N H_2SO_4 in 1N Koh in general were stirred with purified nitrogen. The applicability of the potentiostatic method of triangular voltages to show the influence of inhibitors by applying the principle of Wagner-Traut was examined.

(over)

1. Adsorption on porous electrodes
2. Nickel electrodes
3. Platinum electrodes
I. AFSC Projects 7022, 7353, Task 735305
II. Contract No. AF 61(052)-305
III. Technische Hochuschule, Munich, Germany
IV. L. Kandler et al.
V. Grant No. AF EOARDC 61-20
VI. Aval fr OTS
VII. In ASTIA collection

Aeronautical Systems Division, Dir/Materials and Processes, Metals and Ceramics Lab., Wright-Patterson AFB, Ohio.
Rpt Nr ASD-TDR-62-1067, STUDIES OF HYDROGEN AND OXYGEN EVOLUTION AND THE INFLUENCE OF ADSORBED SUBSTANCES. Final report, Mar 63, 52pp. incl. illus., 38 refs.

Unclassified Report

In this report A. C. Measurements of the interface impedance prove to be suitable for studying adsorption phenomena on porous electrodes like platinated platinum and sintered nickel material. The impedance on platinum electrodes was evaluated for 8N H_2SO_4 and 1N KOH solutions. Further investigations dealt with inhibition problems on highly activated porous nickel electrodes. Several alcohols were used as additives to 1N KOH.

The applicability of the potentiostatic method of applying triangular voltages was examined on bright nickel electrodes. The electrolytes 8N H_2SO_4 in 1N Koh in general were stirred with purified nitrogen. The applicability of the potentiostatic method of triangular voltages to show the influence of inhibitors by applying the principle of Wagner-Traut was examined.

(over)

1. Adsorption on porous electrodes
2. Nickel electrodes
3. Platinum electrodes
I. AFSC Projects 7022, 7353, Task 735305
II. Contract No. AF 61(052)-305
III. Technische Hochuschule, Munich, Germany
IV. L. Kandler et al.
V. Grant No. AF EOARDC 61-20
VI. Aval fr OTS
VII. In ASTIA collection